clean technologies

MDPI

Article

Country-Specific Battery Sizing for Intraday Wind and Solar Shifting Across European Power Systems, 2015–2025

Maksym Mykhei [1,*], Marcela Taušová [1], Peter Tauš [1], Katarína Čulková [1], Tawfik Mudarri [2] and Ibrahim Alkhalaf [3]

[1] Institute of Earth Resources, Faculty of Mining, Ecology, Process Control and Geotechnologies, Technical University of Košice, Letná 9, 042 00 Košice, Slovakia; marcela.tausova@tuke.sk (M.T.); peter.taus@tuke.sk (P.T.); katarina.culkova@tuke.sk (K.Č.)
[2] Institute of Logistics and Transport, Faculty of Mining, Ecology, Process Control and Geotechnologies, Technical University of Košice, Park Komenského 14, 042 00 Košice, Slovakia; tawfik.mudarri@tuke.sk
[3] Embrava, s.r.o., Popradská 2416/64C, 040 11 Košice, Slovakia; alkhalaf.ibrahim@gmail.com
* Correspondence: maksym.mykhei@tuke.sk

Abstract

Reliable comparisons of battery storage requirements depend on an explicitly defined flexibility service. We applied a common hourly residual-load shifting rule to 25 European power systems during 2015–2025 (2,409,740 complete country–hours), using daily cyclic state-of-charge accounting, 90% round-trip efficiency, a 90% usable SOC range and independent P99 energy and power sizing. In 2025, nameplate energy spanned 1.28–142.17 GWh, power 0.28–23.36 GW and implied duration 4.43–7.38 h. Median energy relative to mean national load increased from 1.11 h in 2015 to 2.24 h in 2025. VRE penetration showed a positive country- and year-adjusted association with normalized energy (0.042 h per percentage point; country-clustered 95% confidence interval, 0.025–0.059), without supporting causal inference. In a matched temporal-service comparison, 2025 median energy was 2.240 h for the daily specification versus 5.027 h for the weekly specification; the contrast also reflects balancing and aggregation differences. With fixed P99 ratings, continuous SOC replay fully served a median 82.74% of days, compared with 98.08% marginal daily-envelope coverage. These are conditional technical benchmarks, not guaranteed service levels, observed curtailment recovery, economically optimal investments or total national storage requirements.

Keywords: battery energy storage system; battery sizing; intraday energy shifting; residual load; variable renewable energy; state of charge; operational feasibility; European power systems; hourly electricity data

Check for updates

Academic Editor: Nick Papanikolaou

Received: 19 August 2026
Revised: 3 November 2026
Accepted: 16 November 2026
Published: 19 November 2026

Copyright: © 2026 by the authors. Licensee MDPI, Basel, Switzerland. This article is an open access article distributed under the terms and conditions of the Creative Commons Attribution (CC BY) license.

1. Introduction

The expansion of wind and solar generation is reshaping the hourly relationship between electricity supply and demand. Their weather-dependent output may amplify some residual-load fluctuations while reducing others, depending on the technology mix, demand patterns and available flexibility [1–3]. Battery energy storage systems (BESSs) can provide rapid, short-duration flexibility, but the energy and power associated with a given service cannot be inferred from renewable penetration alone [4,5]. They also depend on the chronological coincidence of demand, wind generation and solar generation, so annual renewable shares provide an incomplete basis for comparative battery sizing.

Battery sizing is conditional on the defined service and operating rules. Energy capacity reflects the cumulative state-of-charge excursion, while power capacity reflects charging and discharging rates; their ratio gives the implied storage duration. The resulting estimates depend on the reference used to define the shifting signal, conversion efficiency, usable state-of-charge range, temporal resolution, treatment of unbalanced energy, terminal state-of-charge conditions and transfer horizon [6–9]. At system scale, hydro resources, transmission and other flexibility options can modify the contribution of additional battery storage [10–12]. Here, residual load denotes electricity demand minus contemporaneous wind and solar generation. It is an accounting signal rather than a measure of observed renewable curtailment: charging below a daily residual-load reference may occur even when residual load remains positive. Accordingly, capacities derived from this signal should not be interpreted as physical surplus absorption or total national storage needs.

Previous studies address prospective system planning, plant-level operation, battery aging and market-oriented optimization [13–16]. Related approaches investigate renewable integration through demand forecasting [17] and investment planning for photovoltaic systems with storage [18]. The question examined here is narrower: how a consistently defined, retrospective intraday shifting service translates harmonized hourly load, wind and solar observations into comparable battery energy, power and duration metrics for 25 European power systems over 2015–2025 [19]. A common deterministic dispatch rule targets deviations from the daily median residual load and separately derives P99 energy and power benchmarks under a 24 h cyclic state-of-charge boundary. Supplementary analyses examine continuous-state-of-charge operational replay, reference and parameter sensitivity, alternative temporal boundaries, VRE-profile perturbations and the influence of reconstructed observations on upper-tail estimates. Country- and year-adjusted associations are assessed without causal interpretation. The reported capacities are service-conditioned technical benchmarks, not optimal investments, guaranteed joint service coverage, reconstructed historical battery operation or estimates of overall national storage adequacy.

2. Literature Review and Hypothesis Development

2.1. Battery Sizing for Variable Renewable Energy Integration

Greater wind and solar penetration changes the timing of net electricity demand, but it does not imply a proportional increase in storage requirements. The relevant flexibility signal depends on the coincidence of demand, solar output and wind generation, as well as on the generation mix and existing flexibility resources [1–3,20,21]. Chronological profiles are thus more informative for an explicitly defined shifting service than annual renewable shares alone.

Battery energy storage systems (BESSs) can provide fast, short-duration responses, yet their sizing depends on the application. Renewable-energy shifting, reserves, congestion support, peak reduction and market participation impose different dispatch and availability requirements [4,22–27]. A configuration suited to balancing services need not be appropriate for renewable firming, autonomous operation or price arbitrage [6,7,16,28–30]. Consequently, no single battery capacity can be regarded as a service-independent national requirement.

Published methods range from residential and plant-level photovoltaic sizing to hybrid wind–solar applications, distribution-system planning and techno-economic optimization [31–39]. Other studies consider multi-objective renewable-energy communities, hybrid storage, coordinated wind–battery design and non-linear battery behavior [40–46]. Investment planning for photovoltaic generation and storage addresses a related but distinct optimization question [18]. Generation forecasts and site-specific photovoltaic design likewise affect prospective system planning without determining a unique retrospective storage bench-

mark [17,47]. These approaches differ in objectives, constraints, temporal resolution and system representation; their reported capacities are therefore not directly interchangeable.

At the European scale, transmission, hydropower, curtailment, sector coupling and alternative storage technologies influence the capacity selected in integrated system models [8–13,48]. Battery–hydropower combinations and other hybrid configurations illustrate that electrochemical storage can complement rather than replace existing flexibility [49–52]. Large-scale storage and hydrogen pathways operate across different timescales and technological boundaries [53–58]. Research on methane-related energy carriers and biogas-mixture safety concerns additional energy-system pathways, not direct evidence of BESS sizing [59,60]. Market and regulatory arrangements further affect which flexibility services can be delivered or remunerated [61]. In this study, national residual load is deliberately defined as load minus wind and solar generation. It is neither observed renewable curtailment nor a net balancing requirement after hydro dispatch and cross-border exchanges; charging can be prescribed while residual load remains positive.

2.2. Temporal Boundaries, Battery Characteristics and Cross-Country Comparability

Chronological battery sizing is sensitive to both the service definition and the method used to close the state-of-charge (SOC) balance. Energy capacity relates to cumulative SOC excursions, while power capacity relates to charging and discharging rates; their ratio expresses the implied storage duration [6,8,62–64]. Temporal aggregation, reference selection and boundary conditions may therefore change the estimated energy benchmark even when the underlying hourly observations are unchanged.

A daily cyclic SOC boundary limits net energy transfer between days; a longer cyclic window permits interday compensation but defines a different service. Multi-period operation, stacked applications and market-oriented dispatch use alternative horizon and terminal conditions [7,16,65]. Larger SOC excursions may arise under longer horizons, although the magnitude and direction of a reported percentile comparison also depend on aggregation and reference rules. Accordingly, a matched 24 versus 168 h comparison should not be described as a pure SOC-boundary experiment or evidence about seasonal storage.

Round-trip efficiency, usable SOC fraction and operational limits affect the conversion from a requested shifting trajectory to a battery nameplate rating [66–68]. Joint interpretation of energy, power and duration is therefore preferable to considering GWh alone [69–71]. However, separately selected upper quantiles of energy and power do not establish their joint operational reliability. A fixed-capacity chronological replay is required to quantify unmet requests, served energy and fully served periods; neither an energy-only percentile nor an unconstrained reference trajectory provides that validation.

Operational intensity is also distinct from lifetime. Equivalent full cycles and power-to-energy ratios characterize a modeled duty profile, while state-of-health evolution additionally depends on temperature, chemistry, SOC trajectory, depth of discharge and calendar aging [15,72–75]. Such indicators cannot by themselves establish a battery's degradation rate, safety performance or economic life.

National comparisons must further distinguish absolute system scale from relative flexibility intensity. European studies show heterogeneous renewable development, resource profiles and storage outcomes [1,9,10,20,76–79]. Cross-country research in other domains likewise illustrates the descriptive value of distinguishing common indicators from country-specific structural conditions, without providing evidence about batteries themselves [80–82]. Here, absolute GWh and GW results are therefore complemented by normalization against average load, peak demand and population. Normalization improves comparability but does not remove differences in system composition or identify their causal contributions.

2.3. Research Gap and Hypotheses

Battery sizing is an established field encompassing system optimization, market operation, economic assessment and degradation-aware design [4,5,14,15,26,34,35]. The contribution sought here is not a new optimal-dispatch algorithm or a claim that no European storage comparisons exist. Rather, it is a reproducible retrospective comparison in which one clearly bounded intraday shifting rule is applied to harmonized historical hourly load, wind and solar profiles, including documented reconstruction where necessary, across a common set of countries and years.

This distinction matters because an optimum obtained with transmission expansion, multiple flexibility technologies or electricity-market revenues answers a different question from a technical benchmark conditional on one dispatch rule [8,11–13,29,30]. The analysis covers 25 European power systems in 2015–2025, reports energy and power requirements as separately estimated P99 benchmarks, and derives duration and system-normalized measures. Complementary checks address continuous-SOC operation with fixed P99 capacities, reference and parameter sensitivity, matched temporal definitions, photovoltaic–wind profile perturbations, data provenance in upper-tail estimates and country–year-adjusted associations. Evidence from reliability-oriented research in other infrastructure domains reinforces the general distinction between nominal indicators and realized service, but is not used as battery validation [83,84].

The following hypotheses concern associations and differences within this specified modeling framework:

H1. *Higher VRE penetration is positively associated with a higher battery-energy benchmark relative to average national load under a common intraday shifting service.*

H2. *Applying identical battery-sizing assumptions across European power systems produces substantial cross-country heterogeneity in battery energy, power and implied storage duration.*

H3. *Under matched hourly observations, extending the represented energy-transfer service from 24 to 168 h is associated with a higher median country-level battery-energy benchmark.*

H1 is an observational, model-conditioned association rather than a causal estimate of the effect of VRE deployment. H2 does not identify economically optimal national installations, and H3 compares specified service horizons rather than long-duration or seasonal adequacy. In particular, independent P99 ratings should not be read as a guarantee that a single continuously operated BESS satisfies every requested charging and discharging interval. All reported capacities remain conditional technical benchmarks, not observed historical storage operation or total national BESS needs.

3. Methodology

3.1. Study Design and Data

This study provides a harmonized retrospective comparison of a predefined battery-flexibility service across 25 European electricity systems during 2015–2025. Identical chronological dispatch, state-of-charge (SOC) accounting and sizing rules were applied to each country–year. Unlike least-cost capacity-expansion or market-optimization studies, the analysis does not seek an optimal storage investment; it estimates technical benchmarks conditional on observed hourly load, wind and solar profiles and a specified operating rule [4,6,16,29,33].

Hourly actual total load (ENTSO-E document A65) and generation by production type (A75) were obtained from the ENTSO-E Transparency Platform [19]. The variable

renewable energy (VRE) signal comprises solar PV (B16), offshore wind (B18) and onshore wind (B19). Hydropower was retained in the underlying technology data but not included in the VRE signal. Eurostat population observations were used for per capita indicators, with World Bank data serving only as a country–year fallback; no population interpolation was performed [85,86].

Electricity series were aligned to a common hourly UTC grid. The S25 sample comprises Austria, Belgium, Bulgaria, Switzerland, Czechia, Germany, Denmark, Estonia, Spain, Finland, France, Greece, Hungary, Ireland, Italy, Lithuania, Latvia, the Netherlands, Norway, Poland, Portugal, Romania, Sweden, Slovenia and Slovakia. Inclusion required at least 95% annual completeness of the model inputs in every year after the predefined validation and reconstruction procedure. Of 2,410,800 expected country–hours, 2,409,740 had complete final battery-model inputs (99.956%). The nested S21 and S12 samples provide stricter data-completeness comparisons.

Available observations were retained. Missing load intervals of at most six consecutive hours and generation gaps of at most two hours were eligible for linear interpolation; longer gaps were reconstructed using validated country-specific or donor-series approaches subject to blocked cross-validation. Unresolved values were not replaced during battery modeling. The baseline uses only complete 24 h UTC days. The processed dataset also retains observed/final values and imputation or provenance indicators, permitting separate upper-tail diagnostics. Figure 1 summarizes the workflow from data harmonization and residual-load construction to dispatch, sizing and robustness analysis.

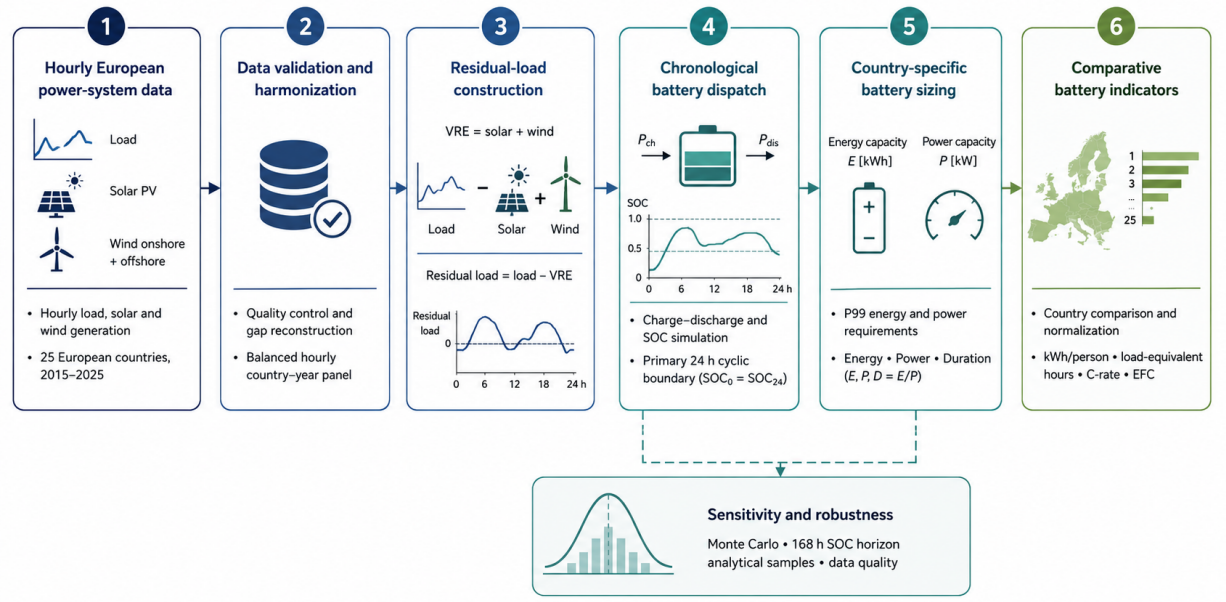


Figure 1. Analytical workflow for deriving country-specific battery energy, power, duration and operating-intensity indicators from harmonized hourly electricity-system observations.

3.2. Chronological Battery Model

Chronological accounting is necessary because storage requirements depend on the order of charging and discharging opportunities, not only their annual totals [4,6,64,69]. For country c and UTC hour t, VRE generation and residual load are defined as

$$\begin{aligned} G_{c,t}^{VRE} &= G_{c,t}^{SOL} + G_{c,t}^{WOF} + G_{c,t}^{WON}, \\ RL_{c,t} &= L_{c,t} - G_{c,t}^{VRE}. \end{aligned} \tag{1}$$

This residual-load series is an accounting construct, not observed curtailment, physical surplus or net demand after cross-border exchanges and other flexibility resources. For

each complete UTC day d, the baseline reference is the median hourly residual load, and potential battery charging and discharging are

$$\begin{aligned} R_{c,d} &= \text{median}(RL_{c,t} : t \in d), \\ \widetilde{C}_{c,t} &= \min\left[G_{c,t}^{VRE}, \max(R_{c,d} - RL_{c,t}, 0)\right], \\ \widetilde{D}_{c,t} &= \max(RL_{c,t} - R_{c,d}, 0). \end{aligned} \tag{2}$$

The rule precludes simultaneous charging and discharging and caps charging by contemporaneous VRE generation. Nevertheless, charging may be requested at positive residual load whenever that load is below the daily reference. It therefore represents a counterfactual shifting service, not charging exclusively from historically curtailed renewable electricity.

The baseline assumes round-trip efficiency $\eta_c\eta_d = 0.90$, with $\eta_c = \eta_d = \sqrt{0.90}$ [15,66,67]. To close each daily SOC cycle, potential charging and discharging are scaled down, never up. Writing $\widetilde{C}_\Sigma = \sum_{t\in d} \widetilde{C}_{c,t}\Delta t$ and $\widetilde{D}_\Sigma = \sum_{t\in d} \widetilde{D}_{c,t}\Delta t$, the non-degenerate scaling factors are $s_C = \min\{1, \widetilde{D}_\Sigma/(\eta_c\eta_d\widetilde{C}_\Sigma)\}$ and $s_D = \min\{1, \eta_c\eta_d\widetilde{C}_\Sigma/\widetilde{D}_\Sigma\}$. Thus, $C_{c,t} = s_C\widetilde{C}_{c,t}$ and $D_{c,t} = s_D\widetilde{D}_{c,t}$; both are zero if either potential-energy total is zero. This enforces $\eta_c \sum C_{c,t}\Delta t = \sum D_{c,t}\Delta t/\eta_d$, while explicitly leaving part of the potential charge or discharge request unserved when balancing requires truncation.

SOC then evolves in stored-energy units as

$$SOC_{c,t} = SOC_{c,t-1} + \eta_c C_{c,t}\Delta t - \frac{D_{c,t}\Delta t}{\eta_d}, \qquad SOC_{c,d,24} = SOC_{c,d,0}, \tag{3}$$

where $\Delta t = 1$ h. The daily cyclic condition intentionally disallows net interday energy transfer. For each day, the usable energy requirement is the range of the complete SOC trajectory, including its initial state. The corresponding nameplate requirement is $E_{c,d}^{nom} = E_{c,d}^{use}/0.90$, using a baseline usable SOC fraction of 90%. These are modeling assumptions rather than chemistry-specific operating limits; alternative parameters and longer terminal horizons are evaluated separately [6,8,63,65].

3.3. Battery Sizing and Comparative Indicators

Country–year design values are empirical upper-quantile summaries of the daily requirements rather than the maxima of all observed days [4,30,31,70]. The baseline applies independent type-7 P99 quantiles to nameplate energy and the larger daily charging/discharging power:

$$\begin{aligned} E_{c,y}^{*} &= Q_{0.99}\left(E_{c,d}^{nom}\right), \\ P_{c,y}^{*} &= Q_{0.99}(P_{c,d}), \\ H_{c,y}^{*} &= \frac{E_{c,y}^{*}}{P_{c,y}^{*}}. \end{aligned} \tag{4}$$

The resulting $(E_{c,y}^{*}, P_{c,y}^{*})$ pair summarizes two marginal requirement distributions; it is neither a jointly observed operating point nor a 99% reliability guarantee for one continuously operated battery. $H_{c,y}^{*}$ is the implied nameplate duration, not the duration of a selected extreme day. Empirical joint daily-envelope coverage is reported separately from operational replay performance.

Absolute energy and power are complemented by nameplate energy per capita, power relative to annual peak load and the normalized energy benchmark

$$H_{c,y}^{load} = \frac{E_{c,y}^{*}}{\overline{L}_{c,y}}, \tag{5}$$

where $\overline{L}_{c,y}$ is mean national load over complete model-input hours. Equivalent power-to-energy ratio and annualized discharge-based equivalent full cycle (EFC) describe the imposed duty; EFC uses the mean daily discharge over modeled complete days, scaled to 365 days and divided by P99 nameplate energy. These measures do not predict battery lifetime, degradation or state of health, which also depend on chemistry, temperature, SOC history, cycle depth and calendar aging [15,72,73,75].

3.4. Hypothesis Assessment and Robustness Analysis

For H1, VRE penetration is annual wind-plus-solar generation divided by annual electricity load; the dependent indicator is P99 nameplate energy relative to mean load. Pooled Spearman association and the cross-country association of 2015–2025 changes provide descriptive comparisons. To address between-country heterogeneity and common annual influences, complementary ordinary least-squares panel models include country and year fixed effects, with country-clustered standard errors and alternative year/two-way clustering. Specification checks use absolute energy and VRE generation, with and without annual load, to assess sensitivity to the shared normalization denominator. Leave-one-country-out and block-bootstrap diagnostics assess coefficient stability. None of these observational associations identifies a causal effect of VRE penetration on battery capacity. The distinction between national and common developments is also relevant to wider European comparative research [87,88].

H2 is examined through the cross-country distributions, rankings and dispersion of energy, power, duration and normalized indicators under the same service assumptions. H3 compares identical complete Monday–Sunday UTC weeks under daily (24 h) and weekly (168 h) cyclic operation. The hourly observations and daily residual-load references are held fixed, but energy balancing and SOC closure differ. The corresponding P99 criteria apply to daily and full-week requirement distributions, respectively. A four-definition decomposition distinguishes (A) daily balancing and daily P99, (B) daily balancing with P99 of weekly maxima, (C) weekly balancing with P99 of within-week maxima of daily excursions and (D) weekly balancing with P99 of full-week SOC excursions. Thus, the 24/168 h contrast changes the represented service and sizing horizon, not solely the terminal SOC constraint [5,8,13,65].

Baseline parameter sensitivity uses 2000 Monte Carlo draws: round-trip efficiency $\{0.85, 0.90, 0.95\}$ with probabilities $\{0.25, 0.50, 0.25\}$; reference residual-load quantile $\{0.40, 0.50, 0.60\}$ with the same weights; design percentile $\{0.95, 0.99, 0.995\}$ with probabilities $\{0.20, 0.60, 0.20\}$; and a triangular usable-SOC fraction on $[0.80, 0.95]$ with mode 0.90. Additional tests compare the daily median with mean, zero and alternative-quantile references, vary assumed parameter weights and ranges, and examine one-factor and interaction sensitivity. A zero-reference case without two-sided shifting opportunities is retained as a non-operating diagnostic, not a practical dispatch comparator. The resulting ranges are conditional *parameter-sensitivity intervals*, not statistical confidence intervals or predictive distributions. Related research illustrates the importance of separating nominal estimates from operational uncertainty, but does not validate the present battery model [83,84].

Operational feasibility is checked independently by reconstructing the baseline requested dispatch and replaying it chronologically with fixed P95, P99 and P100 energy/power ratings, physical SOC and power limits, and no daily SOC reset. The standard replay starts at 50% of usable SOC within each uninterrupted data segment; a two-day diagnostic and a separate retrospective common-SOC-offset test illustrate the importance of the initial SOC. Outputs distinguish marginal P99-envelope coverage, fully served days, delivered energy and unmet requests. Replay results quantify service attainment for these historical targets, not prospective reliability or optimized dispatch.

Further checks compare S25, S21 and S12, restrict days to non-imputed or strictly observed inputs, and test UTC starts at 00:00, 06:00, 12:00 and 18:00 alongside representative local standard and civil-time boundaries. Non-24 h daylight-saving-transition days are excluded from the civil-time specification. To assess sampling sensitivity separately from Monte Carlo parameter variation, 1000 season-stratified resamples of complete Monday–Sunday UTC weeks were generated for each country in 2025 (48–51 eligible weeks). The daily 24 h and weekly 168 h P99 energy and power estimates were recomputed, and empirical 2.5th–97.5th percentile ranges were retained as conditional resampling diagnostics. For 2025, controlled solar/wind energy-share changes of ± 5 percentage points (where identifiable) and within-day wind-profile shifts of ± 6 h retain total VRE energy and the matched daily sample; these are diagnostic perturbations, not forecasts. Finally, imputation flags identify whether P99-tail days contain reconstructed inputs, while clean-day comparisons test sensitivity to sample selection. This provenance analysis is not a direct measurement of reconstruction error or a blocked gap-injection validation.

3.5. Methodological Specification

Figure 1 presents the six-stage analytical workflow. The compact specification provided in Box 1 complements the figure by summarizing the principal modeling assumptions, sizing criteria, and interpretation boundaries. Detailed validation and robustness results are reported in Appendix A.

Box 1. Common Battery-Sizing Protocol

Data and signal. S25: 25 countries, 2015–2025, hourly UTC; S21/S12: stricter completeness samples. $RL = L - (G^{SOL} + G^{WOF} + G^{WON})$.

Service and dispatch. Daily median residual-load reference; VRE-limited potential charging; efficiency-adjusted daily energy balancing; 24 h cyclic SOC. The service is counterfactual, not observed curtailment.

Battery parameters and sizing. Round-trip efficiency 90%, usable SOC 90%; independent empirical P99 nameplate energy and power; implied duration E^*/P^*. These ratings do not guarantee joint service reliability.

Comparability and tests. GWh, GW, duration, normalized capacity and EFC; H1 pooled/change and fixed-effects associations; H2 national dispersion; H3 matched 24/168 h definitions; scenario, time-boundary, data-quality and fixed-capacity replay diagnostics.

Scope. Technical service-conditioned benchmarks, not least-cost investment, optimal dispatch, actual surplus absorption, battery-life prediction or total national storage adequacy.

3.6. Methodological Scope and Limitations

Several limitations bound the interpretation. First, national residual load excludes cross-border flows and the joint dispatch of hydropower, conventional generation, demand response, hydrogen and competing flexibility resources. These can substitute for or complement BESSs, so the benchmarks are not estimates of incremental national storage needs after existing flexibility has been used [10–13].

Second, the daily balancing rule intentionally truncates unmatched charging or discharging opportunities. Separate empirical P99 energy and power ratings do not ensure joint operational feasibility: continuous-SOC replay measures unmet requests under the chosen initial SOC, limits and historical trajectory, without claiming a reliability target, an optimal controller or a minimum feasible capacity. The 168 h comparison also changes aggregation and balancing rules alongside the interday transfer horizon, and is not evidence about seasonal adequacy.

Third, UTC provides a reproducible common calendar rather than a physically privileged national operating day. Shifted and local boundaries can produce material country-specific differences; civil-time checks exclude days of non-standard length. Both Monte Carlo sensitivity ranges and block-bootstrap intervals remain conditional on the tested assumptions or observations, respectively.

Fourth, completeness thresholds and reconstruction diagnostics do not eliminate possible upper-tail bias. Excluding imputed days changes the evaluated sample and cannot establish the accuracy of the imputed extremes; a dedicated blocked gap-injection experiment would be necessary for that purpose. Neither an out-of-year dispatch test nor independent subhourly (15/30 min) ramping and control validation is provided.

Finally, the model excludes energy-market optimization, investment costs, revenues, replacement decisions, network constraints and laboratory-calibrated electrochemical or thermal dynamics. C-rate and EFC thus describe modeled utilization, not degradation, fire safety or lifetime. The reported charging schedule is counterfactual and cannot establish that electricity was historically curtailed or physically available for charging. All results should be read as *conditional technical battery-sizing benchmarks*, not historical battery operation or universal storage prescriptions. Data processing, battery modeling and statistical analyses were performed in R version 4.5.2.

4. Results

Unless indicated otherwise, results refer to the principal S25 sample and the deterministic 24 h cyclic state-of-charge (SOC) specification. Capacities are technical benchmarks for the defined intraday wind-and-solar shifting service, not economically optimal installations, observed battery operation or national storage-adequacy requirements. Supplementary analyses distinguish these unconstrained sizing benchmarks from the service attainable by a single battery with fixed ratings.

4.1. Analytical Coverage and Modeled Intraday Battery Operation

The balanced 2015–2025 panel contains 25 countries, 275 country–years and 2,410,800 expected country–hours. Complete final model inputs were available for 2,409,740 h (99.956%). Battery dispatch was calculated only for complete 24 h UTC days, retaining the distinction between observed, reconstructed and unresolved observations. The nested S21 and S12 samples were examined separately for completeness-related robustness.

Figure 2 illustrates the deterministic rule using the predefined representative 2025 country–day: the country closest to the cross-country median normalized P99 energy benchmark and a day near the 90th percentile of its daily usable-energy requirement. Charging occurs when residual load falls below the daily median reference, subject to the contemporaneous VRE cap, and discharging occurs above that reference. As residual load can remain positive during charging, the illustrated trajectory is a counterfactual shifting request rather than observed renewable-curtailment recovery. Conversion-adjusted balancing closes the daily SOC cycle by reducing potential charging or discharging requests. Across the 25 national systems in 2025, the median country-level fractions of potential charging and discharging energy retained after this balancing step were 76.23% and 77.52%, respectively. The remaining potential energy was not included in the cyclic shifting target. These fractions concern the balancing rule before battery sizing and are distinct from losses during subsequent fixed-P99 replay. The plotted trajectory is not a continuous-year replay of a battery restricted to its P99 ratings.

The illustration also separates the underlying sizing dimensions: peak hourly charge/discharge determines the daily power requirement, while cumulative SOC excursion determines usable energy. Thus, high power over a short interval need not imply a correspondingly large energy inventory.

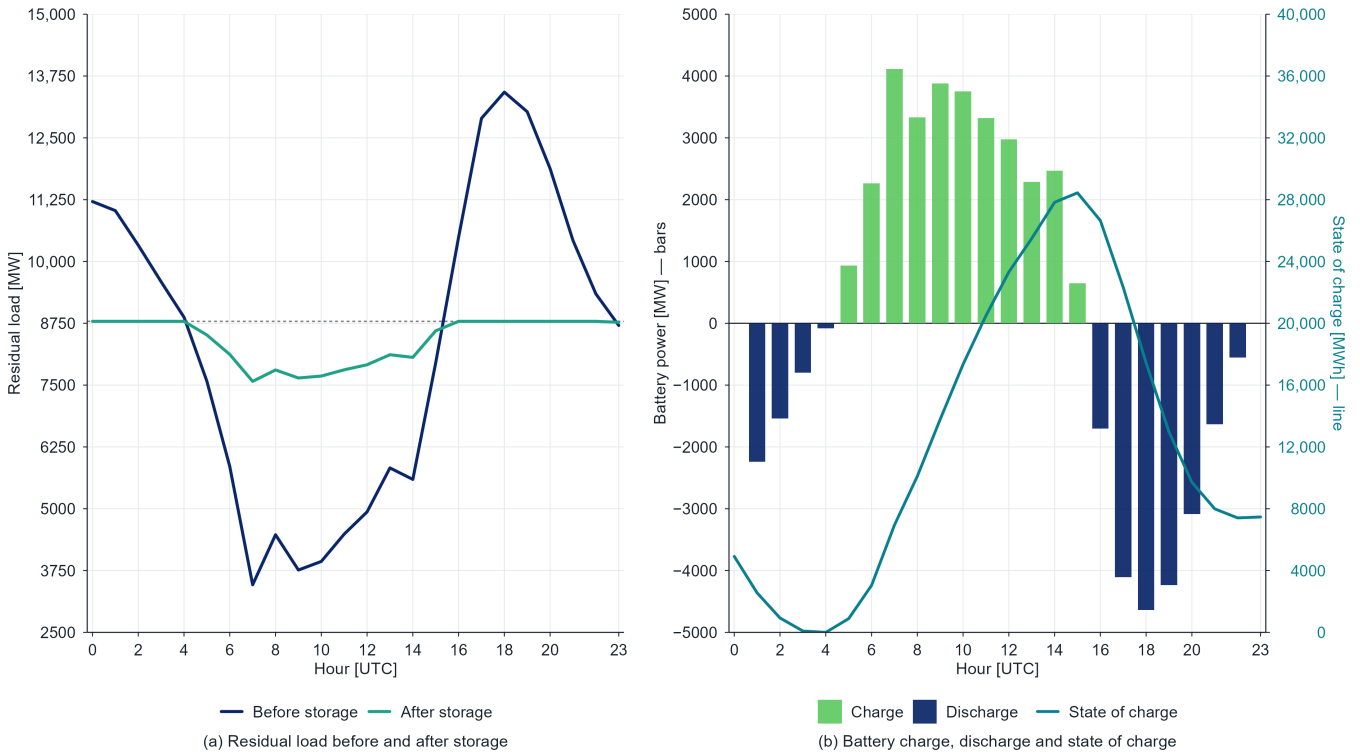


Figure 2. Illustrative deterministic intraday dispatch for the representative 2025 country–day. Panel (**a**) shows residual load relative to its daily reference before and after the modeled shifting rule; panel (**b**) shows charging, discharging and cyclic SOC. The dotted horizontal line in panel (**a**) indicates the daily median residual-load reference. Charging is capped by contemporaneous VRE. The trajectory is an unconstrained daily sizing illustration, not a fixed-P99 continuous-operation validation.

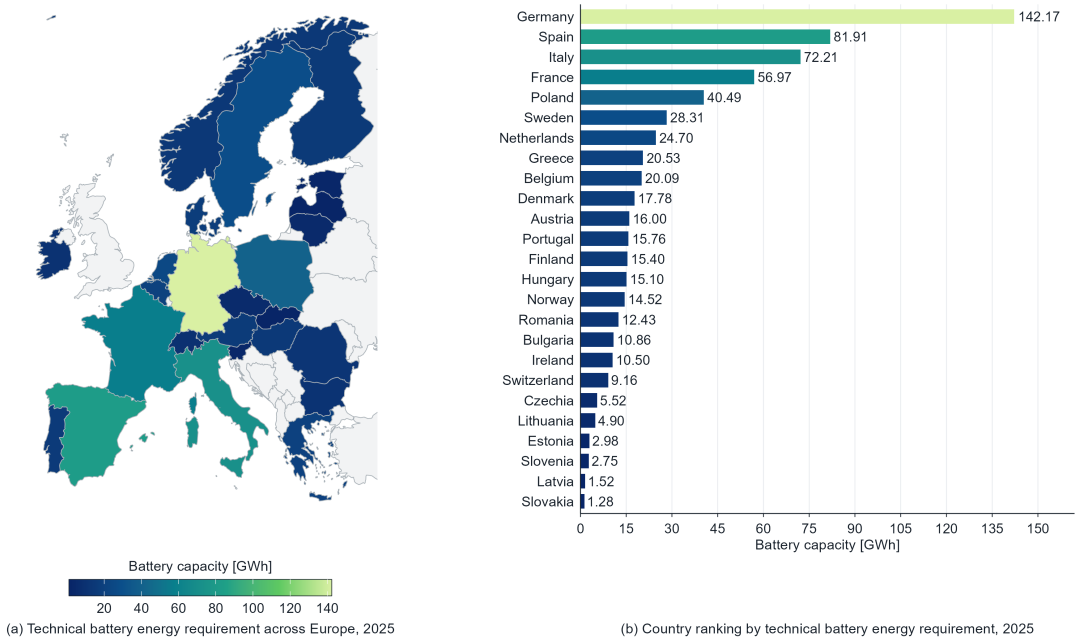
4.2. Country-Specific Battery Energy Requirements in 2025

Applying the same service rule yielded 2025 P99 nameplate-energy benchmarks from 1.28 GWh in Slovakia to 142.17 GWh in Germany, a spread exceeding two orders of magnitude. Figure 3 shows the associated map and country ranking. Germany had the largest absolute benchmark, followed by major electricity systems including Spain, Italy and France; smaller systems generally appeared lower in the absolute ranking.

Differences in absolute GWh combine national electricity-system scale with the timing of demand, wind and solar generation. The map should therefore not be interpreted as a geographic gradient in storage necessity or as evidence that the highest absolute-capacity countries require the highest relative battery intensity. Normalized comparisons are reported in Section 4.4.

4.3. Battery Power and Storage Duration

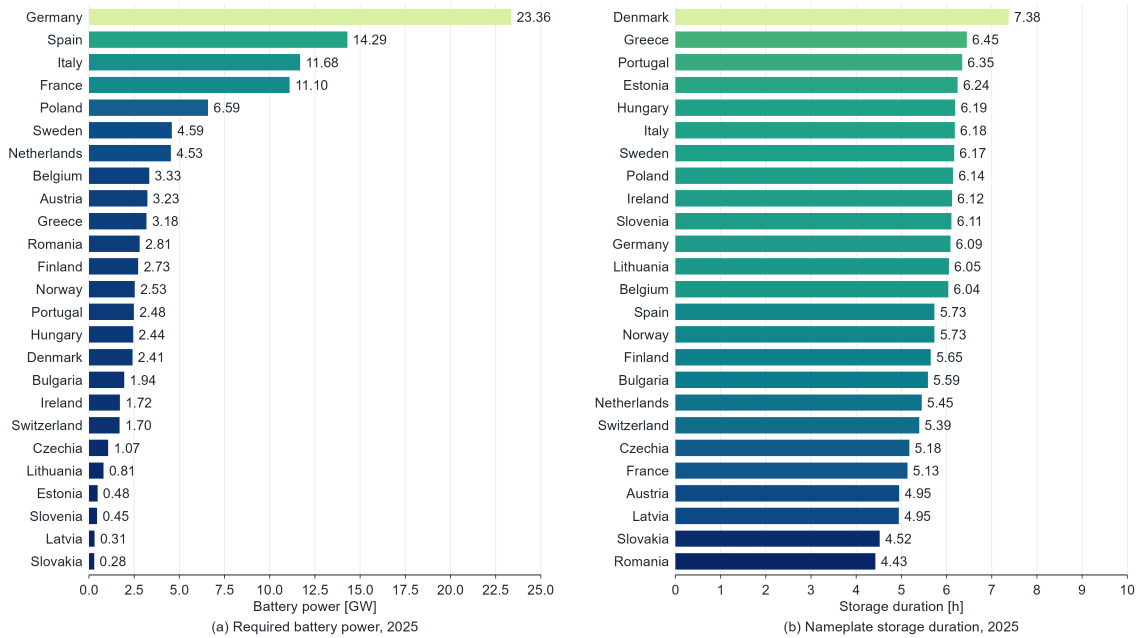
The corresponding 2025 P99 power benchmarks ranged from 0.28 GW in Slovakia to 23.36 GW in Germany (Figure 4a). Spain, Italy and France followed at approximately 14.29, 11.68 and 11.10 GW, respectively; the remaining countries were below 7 GW. Power and energy rankings were not identical because the former reflects hourly transfer rates while the latter reflects accumulated SOC excursions.



(a) Technical battery energy requirement across Europe, 2025

(b) Country ranking by technical battery energy requirement, 2025

Figure 3. Country-specific 2025 P99 nameplate battery-energy benchmarks under the common 24 h shifting service. The map and ranking report absolute energy in GWh; they do not depict observed installations or system-wide storage needs.



(a) Required battery power, 2025

(b) Nameplate storage duration, 2025

Figure 4. Country-specific 2025 battery power and implied nameplate duration. Panel (**a**) ranks independently estimated P99 power; panel (**b**) reports the ratio of P99 nameplate energy to P99 power. The two quantiles need not occur on the same day.

Implied nameplate duration, calculated as the ratio of the independently estimated P99 energy and power values, ranged from 4.43 h in Romania to 7.38 h in Denmark (Figure 4b). Most country values lay near 5–6.5 h, much less dispersed than absolute GWh and GW. These are ratios of marginal upper-quantile ratings, not durations of individual extreme days. Together, the results are consistent with H2: a common service rule yields heterogeneous national energy and power benchmarks without implying heterogeneous economically optimal battery fleets.

4.4. Population- and Load-Normalized Battery Requirements

Normalization changed the 2025 country ranking substantially. Battery energy per capita ranged from approximately 0.24 kWh/person in Slovakia to 2.97 kWh/person in Denmark (Figure 5a). Finland, Sweden and Norway also recorded comparatively high values of 2.73, 2.67 and 2.60 kWh/person, respectively, despite not dominating the absolute GWh ranking.

Energy relative to mean national load ranged from 0.44 h in Slovakia to 4.05 h in Denmark, with a cross-country median of 2.24 h (Figure 5b). Lithuania and Greece reached approximately 3.65 and 3.58 h. Germany's large absolute capacity therefore did not translate into the highest relative intensity. These denominators distinguish system scale from modeled service intensity but do not remove differences in generation composition or prove a causal explanation for country rankings.

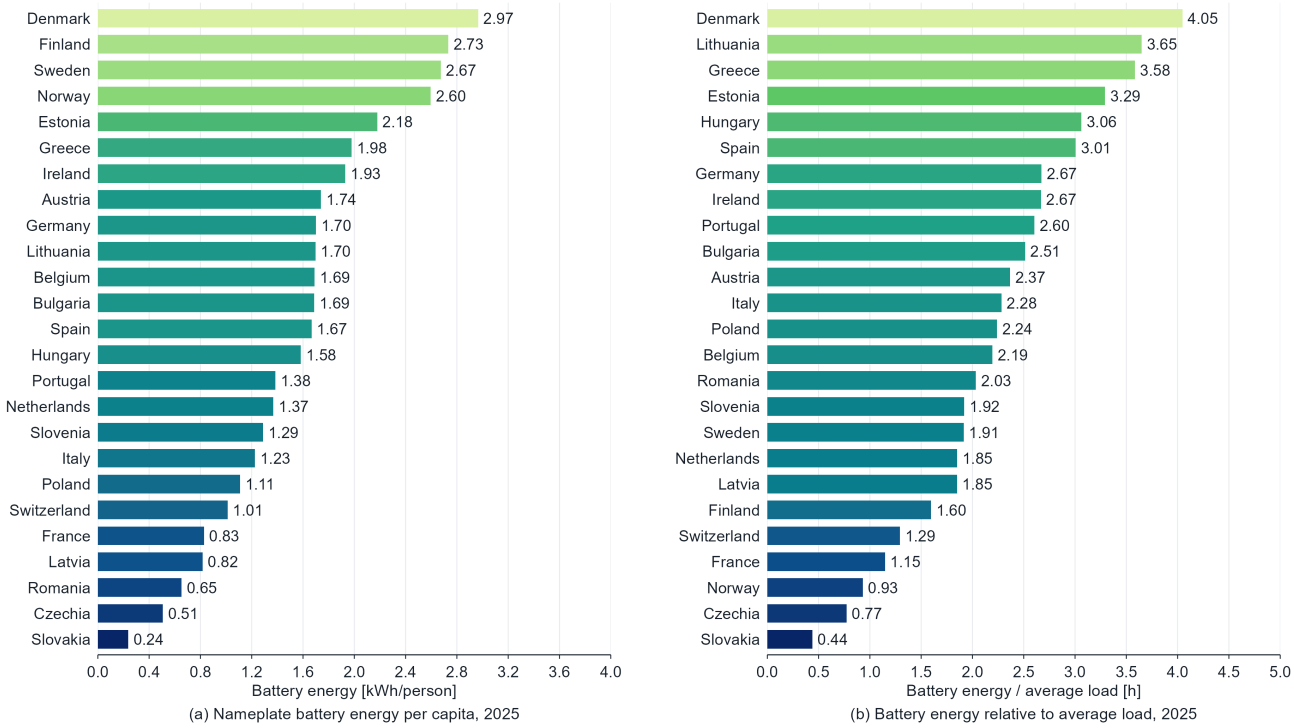


Figure 5. Normalized 2025 P99 nameplate energy: (**a**) kWh per resident and (**b**) average-load-equivalent hours. Rankings are calculated separately for the two denominators and describe different comparative perspectives.

4.5. Evolution of Normalized Battery Requirements, 2015–2025

Figure 6 shows the full 275 country–year series and national trajectories. The cross-country median of nameplate energy relative to mean load increased from approximately 1.11 h in 2015 to 2.24 h in 2025, with heterogeneous, non-monotonic country paths and a wider distribution in later years. Because the metric is load-normalized, the pattern is not solely a consequence of differences in absolute system size; it remains conditional on the selected shifting rule and changing observed profiles.

Across all country–years, VRE generation relative to electricity load and normalized battery energy were positively associated (pooled Spearman $\rho = 0.897$). The correlation of country-specific 2015–2025 changes was weaker ($\rho = 0.495$). A complementary panel regression with country and year fixed effects retained a positive coefficient of 0.042 h of average load per percentage-point increase in VRE penetration (country-clustered 95% confidence interval: 0.025–0.059; $n = 275$). The association remained positive in an absolute-

capacity specification controlling for annual load, and leave-one-country-out estimates did not change its sign. These checks strengthen the descriptive evidence for H1 while neither establishing causality nor attributing the association to a single mechanism. Detailed regression estimates and uncertainty diagnostics are provided in Appendix A.

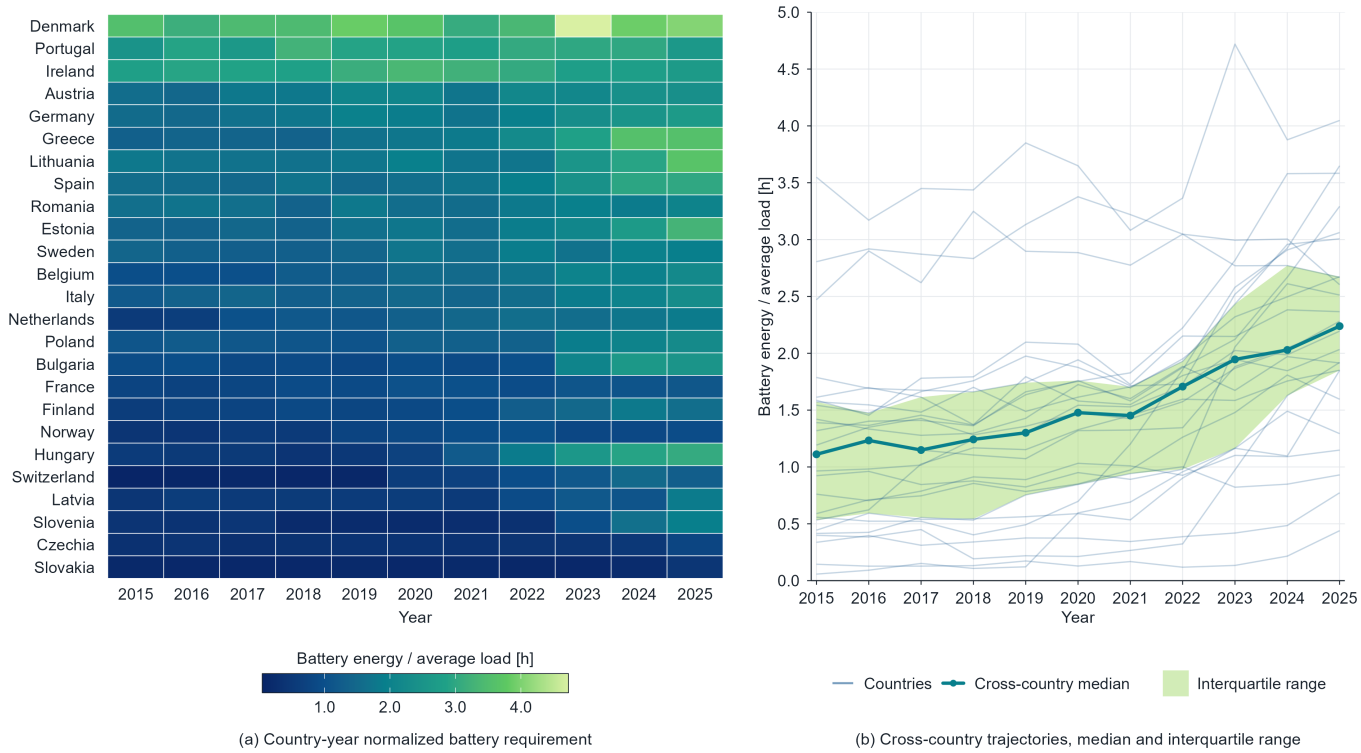


Figure 6. Normalized P99 battery-energy benchmarks during 2015–2025. Panel (**a**) shows the country–year observations; panel (**b**) shows country trajectories and annual cross-country median/interquartile range. The figure is descriptive and does not identify a causal effect of renewable deployment.

4.6. Parameter Sensitivity and Analytical-Sample Robustness

Figure 7a compares each country's deterministic 2025 result with the 2000-draw parameter-sensitivity distribution. The deterministic cross-country median was 2.24 h; under the original parameter weights, the simulation median was 2.26 h and its 2.5th–97.5th percentile interval was 1.69–2.69 h. These are sensitivity bounds, not sampling-confidence intervals or forecasts. The S25, S21 and S12 distributions overlapped substantially (Figure 7b), although changing the country set also changes its geographical composition. A wider parameter-stress specification produced a median of 1.96 h and an interval of 1.07–3.01 h, showing that apparent central stability depends on the tested assumptions.

Reference-rule sensitivity was also material. Replacing the daily median residual-load reference with the daily mean changed the 2025 cross-country median normalized energy from 2.24 to 2.70 h; other quantile references altered country values and rankings. Accordingly, the baseline should be interpreted as one specified service rather than a reference-independent battery requirement.

A separate 2025 operational validation applied the fixed marginal P99 energy and power ratings to continuous chronological SOC replay without daily resetting. Across countries, the median statistical daily P99-envelope coverage was 98.08%, while the median fraction of fully served days in replay was 82.74%. The median achieved share of requested discharge energy was 97.48%. With energy and power limits imposed simultaneously, the cross-country median annualized discharge-based equivalent full cycles decreased from

154.08 EFC/year-equivalent for the unconstrained target to 146.01 for fixed-P99 replay; the median country-level relative reduction was 2.52%. These replay figures refer to actual delivered energy within the modeled 2025 service, not projected battery aging. Thus, the capacity pair can serve most modeled energy while failing to meet the full requested trajectory on some days; marginal quantile coverage is not a joint operational reliability guarantee. Additional P95/P100 and initial-SOC diagnostics are reported in Table A3 in Appendix A.

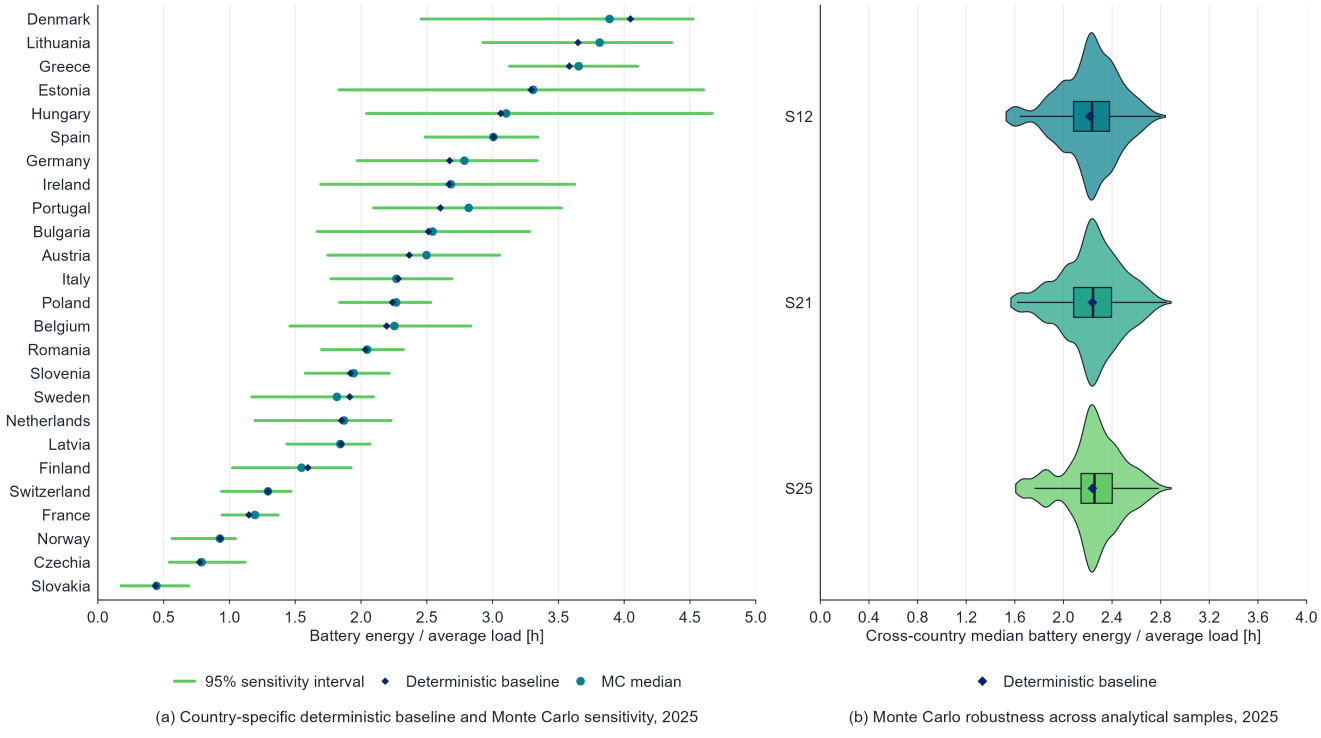


Figure 7. Original 2025 Monte Carlo parameter sensitivity and sample comparison. Panel (**a**) displays country-specific deterministic values, simulated medians and 95% parameter-sensitivity intervals; panel (**b**) shows the S25/S21/S12 distributions of the cross-country median.

4.7. Sensitivity to the Temporal Service Horizon

On identical complete-week observations, the 2025 cross-country median normalized energy increased from 2.240 h for the matched daily specification to 5.027 h for the full-week 168 h specification (Figure 8). This represents a 124.41% increase when calculated from the two country medians; the median of the 25 country-specific percentage changes is 126.12%. These distinct statistics should not be interchanged. The temporal contrast persisted across the study period, with varying country-specific magnitudes.

The comparison changes more than the terminal SOC condition. A four-definition decomposition gave 2025 country medians of 2.240 h (daily balancing/daily P99), 2.385 h (daily balancing/weekly-maximum aggregation), 3.405 h (weekly balancing/within-week maximum daily excursion) and 5.027 h (weekly balancing/full-week SOC excursion). The increase consequently reflects combined changes in balancing, aggregation and permitted energy inventory; H3 concerns these different temporal services, not an isolated boundary-condition effect or seasonal adequacy.

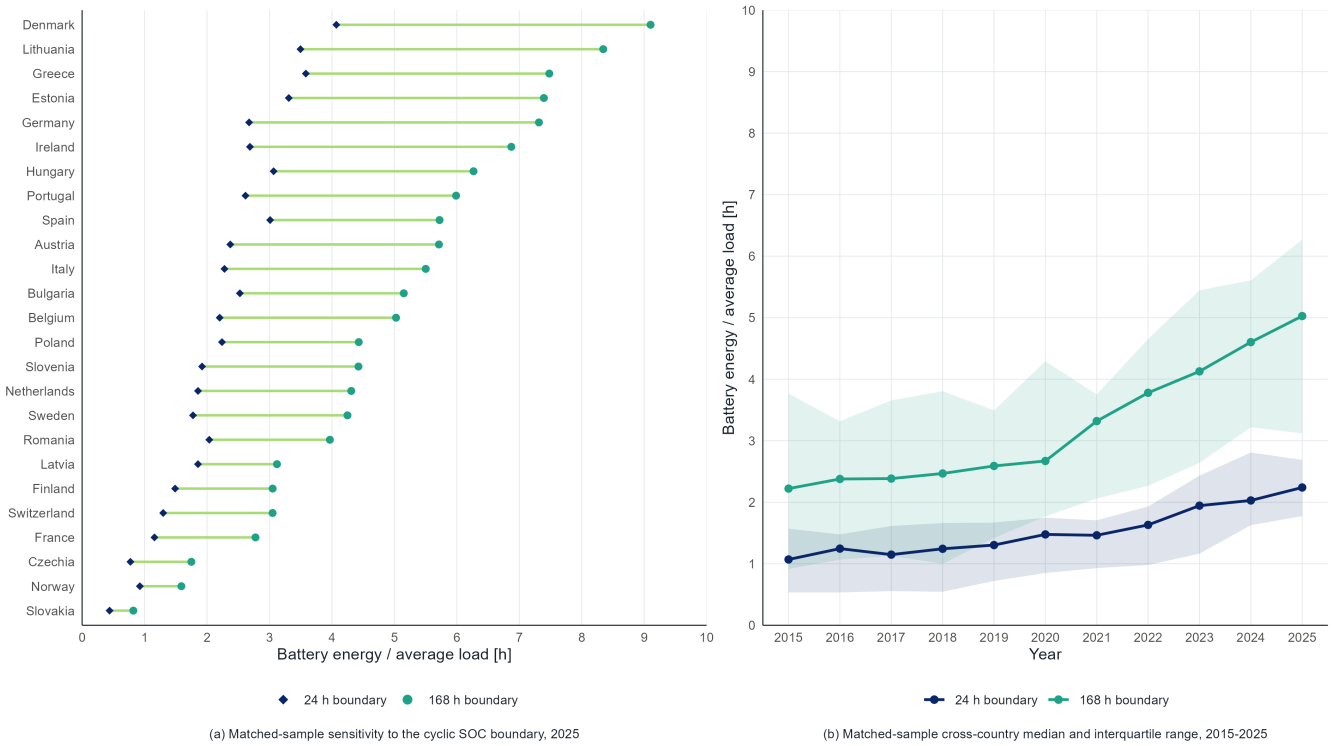


Figure 8. Matched 24/168 h temporal-service comparison. Panel (**a**) presents country-specific normalized 2025 energy and panel (**b**) the annual cross-country median/interquartile range. The same complete-week observations and daily references are used, but balancing, SOC closure and sizing aggregation differ.

The choice of daily clock boundary also matters. Relative to UTC 00:00, shifting the 2025 daily boundary to UTC 06:00 increased Czechia's P99 energy benchmark by 37.38% in the corresponding scenario; other national responses differed. Local civil-time tests exclude non-24 h daylight-saving days. UTC is therefore a reproducible common convention, not an invariant or universally preferred operating boundary. In a separate 1000-draw, season-stratified week-block bootstrap, the median width of the country-specific 2.5th–97.5th percentile intervals for P99 energy was 17.57% of the observed matched-sample value for 24 h operation and 17.62% for 168 h operation; the widest national intervals reached 46.85% and 59.11%, respectively. These describe sensitivity to resampling of the available 2025 weeks, not prospective prediction intervals or out-of-year validation. Temporal and clock diagnostics are documented in Figure A3 in Appendix A and Section A.7.

4.8. Data-Quality Robustness

Removing days with statistically reconstructed battery-model inputs yielded a pooled Spearman rank correlation of approximately 0.998 with the baseline normalized results and a median absolute deviation near 0.18% across the available country–year comparisons. Annual rank correlations were approximately 0.986–0.999. However, the strict-observed variant sometimes retained too few countries for meaningful European ranking comparisons; its restricted samples cannot establish population-wide robustness.

An additional 2025 upper-tail audit showed that reconstructed inputs occurred on P99-tail days in eight countries for the energy metric and eight for the power metric. Across all countries, 16 energy-tail and 15 power-tail country–days contained at least one statistically reconstructed input. Restricting P99 estimation to complete days without statistical imputation changed country energy benchmarks by −7.56% to +2.81% and power benchmarks by −16.12% to +4.14%; the largest negative changes occurred in Spain

for energy and Romania for power. Hence, stable overall rankings do not imply negligible sensitivity of each country's extreme quantiles. Because exclusion changes the evaluated day sample, these differences measure sample sensitivity, not reconstruction error; a blocked gap-injection test remains outside the present validation.

Controlled 2025 profile perturbations provided a further test of temporal dependence at fixed total VRE energy and load. Across comparable countries, reducing the solar share by five percentage points produced a median country-specific energy change of −3.62%, while increasing it by five points yielded +1.37% (24 feasible countries). Shifting within-day wind profiles by −6 and +6 h produced median changes of +1.22% and +2.28%, respectively. Responses varied in sign across countries. These synthetic perturbations assess the baseline service's profile sensitivity, not prospective VRE deployment or causal national effects. Detailed results are provided in Table A8 in Appendix A.

4.9. Battery Operating Intensity and Summary of Principal Results

The 2025 equivalent power-to-energy ratio ranged from approximately 0.14 to 0.23 C, with Romania and Denmark at the respective upper and lower ends. Discharge-based equivalent full-cycle intensity ranged from 60.24 EFC/year-equivalent in Slovakia to 189.67 in Spain; the cross-country median was approximately 154. These indicators describe the unconstrained modeled duty, not electrochemical cycle counts, degradation, state-of-health loss or replacement schedules. Figure A2 in Appendix A provides country-level detail. Table 1 consolidates the principal results, while Tables A1–A8 and Figure A3 in Appendix A document the additional analyses and robustness checks.

Table 1. Principal battery-sizing results and selected validation evidence.

Dimension	Unit	Principal Result	Interpretation
Analytical coverage	%	99.956% of expected country–hours	Complete model inputs across S25
2025 nameplate energy	GWh	1.28–142.17	Absolute country-scale differences
2025 power	GW	0.28–23.36	Independent marginal P99 rating
2025 implied duration	h	4.43–7.38	P99 energy divided by P99 power
2025 energy / mean load	h	Median 2.24; 0.44–4.05	Relative service intensity
2025 energy per capita	kWh/person	0.24–2.97	Population-normalized comparison
2015–2025 cross-country median	h	1.11 to 2.24	Descriptive change in normalized energy
H1 descriptive association	Spearman ρ	0.897 pooled; 0.495 country changes	Positive, noncausal association
H1 country/year fixed effects	h per VRE p.p.	+0.042; 95% CI 0.025–0.059	Country-clustered uncertainty
Monte Carlo, original weights	h	Median 2.26; 95% range 1.69–2.69	Conditional parameter sensitivity
Daily residual-load reference	h	Median 2.24 vs. mean 2.70	Reference choice changes benchmark
Continuous P99 replay, 2025	% of days/energy	98.08% envelope; 82.74% fully served days; 97.48% discharge delivered	Marginal coverage differs from actual service
Sample and country-rank robustness	—	S25/S21/S12 overlap; $\rho \approx 0.998$ without imputation	Does not validate P99-tail reconstruction
Matched 24 vs. 168 h	h	2.240 vs. 5.027 (124.41% median-ratio increase)	Joint change in service and sizing horizon
2025 modeled operating intensity	C; EFC/year	0.14–0.23 C; 60.24–189.67 EFC/year	No battery-lifetime inference

Within the specified retrospective service, the evidence is consistent with H1 as a positive noncausal association, H2 as national heterogeneity under a common rule, and H3 as higher energy benchmarks for the broader weekly service. The continuous-SOC replay and upper-tail diagnostics also delimit these claims: neither independent P99 ratings nor broad rank stability establishes guaranteed service or error-free reconstruction.

5. Discussion

Applying one deterministic shifting rule to 25 European electricity systems yields heterogeneous energy and power benchmarks but a narrower range of implied storage durations. The distinctions between absolute capacity, load-normalized intensity and modeled operating duty are essential: none is a service-independent estimate of national BESS need. The additional validations also qualify the interpretation of the original P99

results. In particular, separate high-quantile energy and power ratings do not ensure that one capacity-constrained battery can deliver the complete requested trajectory.

To clarify the contribution of the present study, Table 2 compares selected storage-sizing approaches according to their analytical scope and principal modeling objective. The comparison concerns research design rather than numerical storage capacities, which are not directly interchangeable across different services, system boundaries and optimization criteria.

Table 2. Comparison of selected previous storage-sizing studies with the present research.

Study	Principal Research Focus	Distinction from the Present Study
Cebulla et al. (2017) [9]	European storage capacity and dispatch under highly renewable energy-system scenarios.	Endogenous system planning and optimization rather than a fixed retrospective intraday shifting rule.
Victoria et al. (2019) [11]	Storage requirements in a networked, sector-coupled European energy system under decarbonization constraints.	Joint representation of multiple sectors and flexibility options rather than a national VRE-based benchmark.
Moser et al. (2020) [8]	Sensitivity of European storage requirements to assumptions and alternative storage technologies.	Technology and system-scenario comparisons rather than one common historical battery service.
Martinez-Rico et al. (2022) [7]	Optimal BESS sizing for hybrid renewable plants participating in electricity and reserve markets.	Plant-level market-oriented optimization, including aging considerations, rather than national chronological benchmarking.
Grimaldi et al. (2025) [14]	Techno-economic optimization of wind-farm battery storage considering arbitrage, curtailment and degradation.	Site-specific investment and operational optimization rather than cross-country comparison under fixed dispatch assumptions.
Present study	Historical hourly comparison of 25 European power systems during 2015–2025 using an identical intraday shifting rule.	Country-specific P99 energy, power and duration benchmarks with operational and robustness diagnostics; no claim of optimal investment or dispatch.

The comparison highlights the complementary role of the present approach. Optimization studies estimate storage configurations within specified technical or economic objectives, while the current framework applies one transparent shifting rule to observed national profiles. Its contribution is therefore comparative consistency across countries and years, not an alternative estimate of the least-cost or physically necessary storage capacity.

5.1. European Heterogeneity and the Evolution of Battery Requirements

The 2025 nameplate-energy benchmarks span 1.28–142.17 GWh and the power benchmarks 0.28–23.36 GW. Germany has the largest absolute values, while Denmark ranks highest after normalization by average load and population. This contrast illustrates why system scale cannot substitute for a measure of relative shifting intensity. The several-hour duration range (4.43–7.38 h) follows from the imposed intraday service; it is neither a demonstrated optimum nor a prescription for standard 1, 2 or 4 h commercial configurations. Storage-sizing studies similarly distinguish the service objective from the resulting power and energy ratings [2,4,5,8,9,12,13,22].

The cross-country median normalized energy increased from approximately 1.11 h in 2015 to 2.24 h in 2025, although national paths were non-monotonic. The pooled VRE–battery Spearman correlation was $\rho = 0.897$, compared with $\rho = 0.495$ for the country-specific 2015–2025 changes. A complementary regression with country and year fixed effects retained a positive coefficient of approximately 0.042 h of mean load per percentage-point increase in annual VRE penetration (country-clustered 95% confidence interval: 0.025–0.059). Its sign remained positive under leave-one-country-out checks and an alternative absolute-capacity specification controlling for annual load. These results support the descriptive direction of H1, but neither the pooled correlation nor the fixed-

effects coefficient identifies a causal response of battery investment to VRE deployment. Both indicators are constructed partly from the same load and renewable-generation data, while the two normalized variables also share a load denominator.

Country differences additionally reflect generation composition and chronological coincidence. In controlled 2025 perturbations preserving total VRE energy and matched demand, changing the solar share by -5 and $+5$ percentage points produced median country-level energy-benchmark changes of -3.62% and $+1.37\%$, respectively; the positive shift was identifiable in 24 countries. Shifting wind profiles by -6 or $+6$ h within days produced corresponding medians of $+1.22\%$ and $+2.28\%$. The sign and magnitude varied among countries. These synthetic tests distinguish some timing and mix sensitivity from changes in total annual VRE energy, but they are neither feasible deployment scenarios nor causal identification experiments. European research likewise documents heterogeneous renewable resource and deployment pathways [1,10,11,76–78].

Accordingly, H2 is supported as heterogeneity within a common service definition. The observed dispersion cannot be attributed uniquely to renewable penetration, generation mix, interconnection or geography without additional controls and system modeling. The study's comparative contribution is the fixed methodological boundary, not a claim to identify the optimal BESS fleet of each country.

5.2. Temporal Service Definition as a Determinant of Battery Energy

The temporal-service comparison is more consequential than a simple choice of numerical solver. On matched complete weeks, the 2025 cross-country median energy benchmark was 2.240 h of average load under daily operation and 5.027 h under the full-week specification. The increase calculated from these two medians is 124.41%; the median of country-specific percentage increases is 126.12%. These statistics describe different aggregations and should not be conflated.

The difference is not attributable solely to relaxing the terminal SOC constraint. A four-definition decomposition yielded cross-country medians of 2.240 h for daily balancing and daily P99, 2.385 h for daily balancing with weekly-maximum aggregation, 3.405 h for weekly balancing with within-week maximum daily excursions, and 5.027 h for weekly balancing with full-week SOC excursions. Consequently, energy-balance rules, the allowable carry-over and the distribution to which P99 is applied jointly influence the comparison; differences between cross-country medians should not be treated as additive country-level effects. This interpretation is consistent with the literature emphasizing temporal resolution, storage-operation horizons and terminal conditions [5,6,8,13,65].

The definition of a daily boundary also matters. Shifting the UTC start or applying local calendar boundaries changed individual national P99 estimates, sometimes materially; daylight-saving transitions require special treatment of non-24 h days. UTC 00:00 remains a transparent convention for international comparability, not a physically invariant operational boundary. Thus H3 concerns the higher benchmark associated with a different weekly energy-transfer and sizing service. It does not imply that the daily model undersizes the same service or that either specification measures seasonal adequacy.

5.3. Robustness and Battery Operating Characteristics

The 2025 deterministic cross-country median (2.24 h) was close to the original 2000-draw Monte Carlo median (2.26 h), with a 95% parameter-sensitivity interval of 1.69–2.69 h. However, a wider parameter-stress exercise gave a median of 1.96 h and a wider interval of 1.07–3.01 h, while replacing the daily median residual-load reference with the mean increased the median benchmark from 2.24 to 2.70 h. Central stability is therefore conditional on the selected operating reference, parameter ranges and sampling weights. These

Monte Carlo intervals represent variation in assumed model parameters, not measurement uncertainty, frequentist confidence intervals or future-system forecasts.

S25, S21 and S12 showed broadly overlapping central distributions. Excluding days with statistically imputed model inputs also preserved the overall country ordering ($\rho \approx 0.998$), with a median absolute normalized-energy deviation near 0.18%. Nevertheless, stability of national ranks must not be confused with validation of reconstructed extreme observations. In the separate 2025 P99-tail audit, imputed inputs appeared on upper-tail days in eight countries for energy and eight for power. Exclusion of imputed days changed individual energy benchmarks by as much as −7.56% and power benchmarks by as much as −16.12%. These differences chiefly reflect a change in the eligible day sample; they do not measure reconstruction error. A blocked gap-injection experiment on originally observed extreme intervals would be needed to test that error directly.

More importantly, the operational replay exposes a distinction hidden by independent P99 sizing. Across countries in 2025, median daily P99-envelope coverage was 98.08%, but a single fixed-P99 battery replayed chronologically without daily SOC resets fully served a median of only 82.74% of days; the median share of requested discharge energy served was 97.48%. Hence, high energy delivery can coexist with incomplete daily service. These are retrospective service-attainment diagnostics under specified initial SOC and power/SOC limits, not loss-of-load probabilities, out-of-year guarantees or results of optimal dispatch. A larger ex-post capacity can increase service attainment, but that does not establish a minimum technically feasible or least-cost design.

The modeled equivalent power-to-energy ratios (0.14–0.23 C) and baseline annualized discharge throughput (60.24–189.67 EFC/year-equivalent) describe the unconstrained shifting target rather than the throughput guaranteed by the final P99 configuration. In the 2025 continuous-SOC replay, median country-level EFC decreased from 154.08 for the unconstrained target to 146.01 under fixed energy and power limits, with a median paired reduction of 2.52%. Neither indicator establishes degradation or lifetime. State of health depends on chemistry, temperature, SOC exposure, cycle depth and calendar aging [15,72,73,75]. Multiscale approaches integrating design, market participation and replacement decisions address questions that the present dispatch rule does not solve [89]. Experimental evidence on thermal-runaway mitigation, thermo-electrically induced failure in large-format lithium iron phosphate cells, and confined-geometry jet flames highlights safety considerations beyond hourly power-system modeling [90–92]. These cell-level studies do not validate or modify the battery-capacity benchmarks estimated here.

5.4. Scope, Limitations and Implications

The national residual-load signal excludes actual cross-border electricity exchanges and does not co-optimize BESSs with reservoir hydro, pumped storage, demand response, conventional generation or hydrogen. Transmission and competing flexibility may reduce or complement the role of batteries, so the derived capacities are not incremental national storage needs after existing resources have been dispatched [8,10–13]. The charging rule is explicitly counterfactual: it may allocate VRE to charging while residual load is still positive. Its output is neither measured curtailment recovery nor a demonstration that the charging electricity was historically available to a real battery.

The study also has no optimization benchmark that minimizes battery capacity or system cost while delivering an exactly matched shifting service. Neither investment costs, market revenues, network constraints, replacement policies nor technology competition enter the sizing objective; profit, net present value and payback are therefore not estimated. Market- and investment-oriented BESS studies consequently provide alternative decision frameworks, not a basis for describing the present P99 values as optimal

[7,14,15,18,28,72]. Forecast-based renewable planning addresses a further distinct question, while the present analysis is historical and deterministic [17]. Moreover, the one-hour data do not resolve 15/30 min ramps or validate inverter controls; no hardware-in-the-loop or laboratory-calibrated electrochemical or thermal-runaway analysis was performed. Sodium-ion batteries are a potential alternative chemistry, and recent hard-carbon anode research addresses sodium-storage performance and interfacial stability at cell level [93]; those results cannot be transferred into the present system-level sizing model without chemistry-specific parameters. These omissions limit physical design, safety and financial interpretations, not the arithmetic reproducibility of the specified benchmark.

Practical deployment decisions also require an institutional and social context that the battery algorithm does not represent. Research on renewable deployment and energy poverty addresses transition pathways and distributional outcomes [94,95]; work on environmental-policy instruments, public environmental spending and ESG-related financial outcomes addresses other dimensions of policy and investment decisions [96–98]. Studies of AI in smart-city administration and citizen science concern public governance and participation rather than BESS dispatch [99,100]. These sources provide *broader context only*: none independently supports the numerical energy or power estimates reported here.

The distinction between technical modeling and application-specific decision objectives also arises outside electricity storage. Research on CNC-machine life cycles, mining-equipment optimization and rolling-mill scheduling addresses different industrial decision problems [101–103]. Conveyor-energy simulations and Industry 4.0 logistics research likewise concern industrial efficiency and organizational systems [104,105]. These are methodological or sectoral parallels, *not* empirical validations of the battery model; their inclusion must not be interpreted as evidence that the derived P99 benchmarks are optimal or physically verified.

Within the stated boundaries, three practical implications follow. Comparative BESS studies should report energy, power and duration jointly, disclose their temporal reference and SOC conditions, and distinguish marginal percentile envelopes from continuous operational service. They should also report both absolute and normalized quantities while acknowledging the role of national profiles and competing flexibility. Finally, empirical-tail provenance and model sensitivity should accompany any country-level extreme benchmark. The principal contribution is a transparent, service-conditioned comparison across observed European hourly profiles, providing a common starting point—rather than a substitute—for later optimal-dispatch, network, market, degradation and subhourly studies.

6. Conclusions

This retrospective study compared a common intraday battery-shifting service across 25 European electricity systems using hourly load, solar and wind observations from 2015 to 2025. Under the 24 h cyclic specification, 2025 P99 nameplate benchmarks ranged from 1.28 to 142.17 GWh for energy and from 0.28 to 23.36 GW for power, with implied durations of 4.43–7.38 h. The cross-country median energy benchmark relative to average load rose from 1.11 h in 2015 to 2.24 h in 2025. Absolute capacity and normalized intensity therefore convey different aspects of the defined service.

Annual VRE penetration was positively associated with load-normalized battery energy (pooled Spearman $\rho = 0.897$; country-specific 2015–2025 changes, $\rho = 0.495$). A country- and year-fixed-effects model retained a positive coefficient of approximately 0.042 h per percentage-point increase in VRE penetration (country-clustered 95% confidence interval: 0.025–0.059). These findings are consistent with H1 but do not identify a causal effect. Country heterogeneity supports H2 within the common service boundary; controlled

solar–wind perturbations further illustrate the sensitivity of the benchmark to generation mix and timing.

Under matched hourly observations, the 2025 median increased from 2.240 h for the 24 h service to 5.027 h for the 168 h service. This equals a 124.41% increase between cross-country medians; the median of country-specific percentage increases was 126.12%. The result is consistent with H3 but combines changes in energy balancing, state-of-charge closure and sizing aggregation, rather than isolating one terminal constraint. Reference-rule and parameter tests likewise show that the benchmark is conditional on its operating assumptions.

The additional validations temper conclusions about practical delivery. In continuous operation with fixed P99 ratings, the median share of fully served days was 82.74%, compared with 98.08% marginal daily-envelope coverage, while 97.48% of requested discharge energy was delivered. Independently estimated P99 energy and power therefore do not guarantee joint operational reliability. Overall country rankings were stable when statistically reconstructed inputs were excluded, but individual upper-tail benchmarks could change; these comparisons do not validate reconstruction accuracy. C-rate and annualized discharge throughput describe modeled duty, not degradation or lifetime.

The reported capacities remain service-conditioned technical benchmarks, not economically optimal installations, observed curtailment recovery or total national storage requirements. Further work should examine matched-service optimization, blocked gap-injection tests, subhourly operation, cross-border exchanges, hydro and other flexibility resources, market valuation and chemistry-specific aging. These extensions would connect the present comparison to physically constrained and investment-oriented battery planning.

Supplementary Materials: The following supporting information can be downloaded at https://www.mdpi.com/article/10.3390/cleantechnol8060195/s1, The Supplementary Materials contain the R scripts used for data acquisition, validation, processing, battery modeling, statistical analysis, and robustness testing.

Author Contributions: Conceptualization, M.M.; methodology, M.M.; software, M.M. and M.T.; validation, M.T., P.T., K.Č., T.M. and I.A.; formal analysis, M.M.; investigation, M.M. and K.Č.; resources, M.T. and K.Č.; data curation, M.M.; writing—original draft preparation, M.M.; writing—review and editing, M.M., M.T.,P.T., K.Č., T.M. and I.A.; supervision, M.T. and P.T.; project administration, M.M., P.T. and M.T. All authors have read and agreed to the published version of the manuscript.

Funding: This research was supported by the Scientific Grant Agency of the Ministry of Education, Research, Development and Youth of the Slovak Republic and the Slovak Academy of Sciences (VEGA), grant number 1/0760/26, and by the Cultural and Educational Grant Agency of the Ministry of Education, Research, Development and Youth of the Slovak Republic (KEGA), grant numbers 075TUKE-4/2024 and 006TUKE-4/2024.

Institutional Review Board Statement: Not applicable. This study was based exclusively on aggregated, publicly available electricity-system and population data and did not involve human participants, identifiable personal data, human biological material or animal subjects.

Informed Consent Statement: Not applicable.

Data Availability Statement: The electricity-system data used in this study were obtained from the ENTSO-E Transparency Platform, including Actual Total Load (A65) and Actual Generation per Production Type (A75). Population data were obtained from Eurostat, with World Bank data used as a fallback for individual country–years where necessary. These data are accessible from their respective providers, subject to the applicable access conditions and terms of use. The R scripts used for data acquisition, validation, processing, battery modeling, statistical analysis and robustness testing will be provided as Supplementary Materials through the MDPI submission system alongside the revised manuscript. The original downloaded datasets and the authors' private API tokens, login credentials and other authentication information are not included in the supplementary package.

Researchers wishing to reproduce the analyses must obtain the source data independently from the original providers and configure their own access credentials where required. Reproduction also requires the necessary R packages and appropriate configuration of the local computing environment.

Acknowledgments: During the preparation of this manuscript, the authors used ChatGPT (OpenAI; GPT-6) to assist with technical translation into English, terminological consistency and grammatical editing. Grammarly was also used for spelling, grammar and language proofreading. The authors reviewed and edited the resulting text and take full responsibility for the scientific content, analyses, interpretations and final manuscript. Neither tool is treated as a source of scientific evidence.

Conflicts of Interest: The authors declare no conflicts of interest. Ibrahim Alkhalaf was employed by Embrava, s.r.o., as disclosed in the author affiliations.

Abbreviations

The following abbreviations are used in this manuscript:

A65	ENTSO-E actual total load data
A75	ENTSO-E actual generation by production type data
BESS	Battery energy storage system
C-rate	Equivalent battery power-to-energy ratio
EFC	Equivalent full cycle
ENTSO-E	European Network of Transmission System Operators for Electricity
EU	European Union
GW	Gigawatt
GWh	Gigawatt-hour
IQR	Interquartile range
kWh	Kilowatt-hour
MW	Megawatt
MWh	Megawatt-hour
P99	99th-percentile design criterion
RTE	Round-trip efficiency
S12	Strict 12-country analytical sensitivity sample
S21	High-completeness 21-country analytical sensitivity sample
S25	Principal 25-country analytical sample
SOC	State of charge
UTC	Coordinated Universal Time
VRE	Variable renewable energy

Appendix A. Additional Analyses

These analyses document sample selection and provide diagnostics for the country–year association, fixed-capacity operation, model assumptions, temporal boundaries and reconstruction provenance. The original matched 24 versus 168 h comparison remains in the main Results section because it defines a substantive comparison of distinct shifting services. The additional results reported here are retrospective tests conditional on the stated data, dispatch and sizing rules. In particular, empirical percentile coverage must not be equated with continuous-service reliability, and sample-exclusion tests must not be equated with validation of imputation accuracy.

Appendix A.1. Composition of the Analytical Samples

The principal S25 panel required at least 95% annual completeness of the validated load and VRE inputs in each year from 2015 to 2025. S21 required at least 99% annual completeness, and S12 was the predefined strictest subset. All three samples were defined independently of the resulting battery capacities. The completeness criteria refer to the

model-ready series following the documented validation and reconstruction procedure, not exclusively to raw, directly observed records.

Table A1. Composition of the predefined analytical country samples.

Sample	*N*	Eligibility	Countries
S25	25	Annual model-input coverage $\geq$ 95% throughout 2015–2025	Austria, Belgium, Bulgaria, Switzerland, Czechia, Germany, Denmark, Estonia, Spain, Finland, France, Greece, Hungary, Ireland, Italy, Lithuania, Latvia, the Netherlands, Norway, Poland, Portugal, Romania, Sweden, Slovenia and Slovakia
S21	21	Annual model-input coverage $\geq$ 99% throughout 2015–2025	Austria, Belgium, Bulgaria, Switzerland, Czechia, Germany, Denmark, Estonia, Spain, Finland, France, Greece, Hungary, Italy, Latvia, the Netherlands, Norway, Poland, Portugal, Slovenia and Slovakia
S12	12	Predefined strictest analytical subset	Austria, Belgium, Bulgaria, Switzerland, Czechia, Denmark, Finland, Greece, Norway, Poland, Portugal and Slovenia

Appendix A.2. VRE Penetration and Country–Year Panel Robustness

Figure A1 retains the original descriptive comparison: 275 country–year observations yield pooled Spearman $\rho = 0.897$, while the association between national 2015–2025 changes is $\rho = 0.495$. Their difference cautions against interpreting pooled spatial variation as a within-country effect. A complementary country- and year-fixed-effects specification, with country-clustered uncertainty, retains a positive partial association (Table A2). The regression is observational; fixed effects do not establish a causal effect of VRE deployment or remove the mechanical relationship arising because both variables are constructed from load and VRE generation.

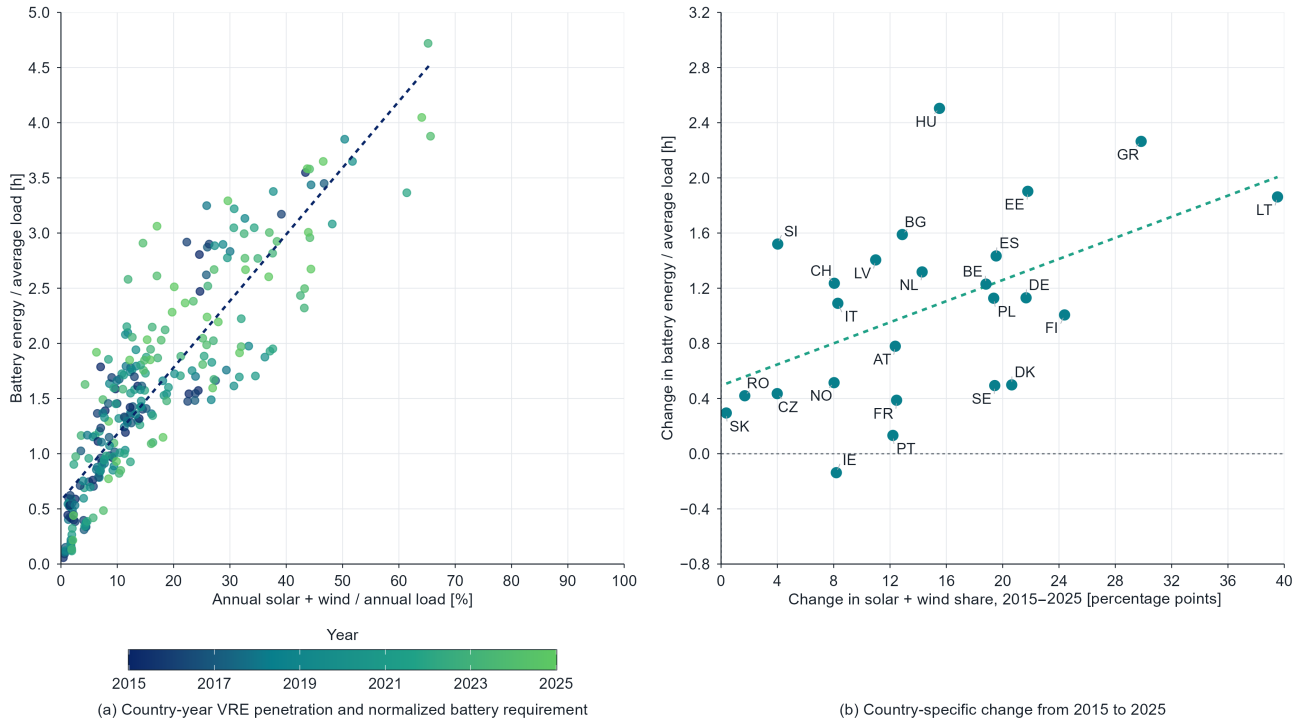


Figure A1. Observed association between annual VRE penetration and the normalized P99 battery-energy benchmark. Panel (**a**) displays 275 country–years; panel (**b**) compares 2015–2025 country-specific changes. Spearman correlations are descriptive and do not identify causation.

Table A2. Selected 2015–2025 H1 association checks (25 countries, 275 country–years).

Specification	Estimate	SE	95% CI Lower	95% CI Upper	Unit/Interpretation
Pooled Spearman	0.897	—	—	—	Rank association
Country-change Spearman (2015–2025)	0.495	—	—	—	Rank association; 25 changes
Country and year FE (M03), country-clustered	0.04198	0.00822	0.02502	0.05894	Average-load-equivalent h per 1 percentage point VRE
Absolute-energy FE with annual-load control (M06), country-clustered	0.51743	0.06914	0.37474	0.66013	GWh battery per 1 TWh annual VRE

The M03 country-clustered test gives $p = 3.16 \times 10^{-5}$ ($t_{24} = 5.108$). Leave-one-country-out M03 estimates remain positive, and country-block bootstrap resampling (499 valid draws) yields a percentile interval of 0.02586–0.05725 h per VRE percentage point. Alternative year and two-way clustering also retain a positive coefficient. These are robustness diagnostics for a conditional association, not causal inference or a prediction of investment requirements.

Appendix A.3. Marginal P99 Sizing Versus Continuous-SOC Service Delivery

Independent daily energy and power percentiles produce a convenient capacity envelope, but do not automatically provide a feasible, continuously operated annual dispatch. A separate 2025 replay applied fixed power and energy ratings to the chronological target trajectory, enforced SOC and power bounds and carried SOC across consecutive days. For the P95, P99 and P100 replay rules, the starting SOC was 50% of usable capacity in each uninterrupted segment; unlike baseline sizing, SOC was then carried between consecutive days. The P100_COMMON diagnostic instead used a retrospective joint-capacity and initial-SOC configuration. Table A3 reports cross-country medians of the national performance measures; it does not pool all country–days into a single reliability statistic.

Table A3. 2025 operational replay: median national coverage and energy-delivery measures across 25 countries (%).

Fixed-Capacity Rule	Marginal Daily Envelope	Fully Served Days in Replay	Requested Discharge Delivered
P95 energy and power	92.88	70.14	95.00
P99 energy and power	98.08	82.74	97.48
P100 energy and power	100.00	92.60	98.87
P100_COMMON (retrospective joint capacity)	100.00	100.00	100.00

The 2025 P99 replay fully served between 68.49% and 93.97% of eligible days across individual countries, compared with a cross-country median of 82.74%. The median national unconstrained and achieved discharge-based intensities were 154.08 and 146.01 EFC/year-equivalent, respectively (median paired national reduction: 2.52%). The median country-level unserved discharge over 2025 was 55.47 GWh; the separately calculated country medians of SOC- and power-clipped discharge were 55.25 and 0.11 GWh, respectively. Medians of separate components need not sum to the median total. Earlier in the processing chain, daily cyclic balancing retained a median of 76.23% of potential charging energy and 77.52% of potential discharging energy. Across the 25 independent 2025 country models, the sums of potential versus balanced charging requests were 156.15 versus 115.75 TWh, while the corresponding discharging requests were 143.10 versus 104.18 TWh. These differences quantify counterfactual potential energy omitted by daily balancing, not physically curtailed renewable electricity. Potential-energy reductions at the balancing stage and unmet requests during capacity-constrained replay are different quantities and must not be added. P100 uses separate daily marginal maxima and is still not a guarantee of full continuous

service. P100_COMMON instead allows a larger retrospective joint capacity with a selected starting SOC and is a diagnostic of the tested historical trajectory, *not* a minimum-capacity solution, an optimal controller or an out-of-year reliability demonstration. Charge energy assigned while residual load was positive was also present in every country, with a median share of 100%; this confirms that the imposed charging signal must not be called observed renewable curtailment.

Appendix A.4. Sensitivity to Statistical Reconstruction and Upper-Tail Provenance

Over the 2015–2025 comparisons for which valid national estimates remained, excluding days with statistically reconstructed battery-model inputs produced pooled Spearman $\rho \approx 0.998$ relative to the full validated baseline, a median absolute deviation near 0.18% in normalized battery energy and annual rank correlations of approximately 0.986–0.999. The stricter requirement of entirely directly observed input hours sometimes left too few countries for meaningful rank comparison. Consequently, these checks support the stability of broad rankings only for the eligible observed subsets.

The 2025 provenance audit examined the days entering the empirical upper tails of the energy and power distributions. Table A4 distinguishes the presence of an imputed input on a P99-tail day from the actual accuracy of the reconstructed value. Re-estimating P99 on complete days without statistical imputation changes the set of eligible days and therefore cannot estimate reconstruction error directly.

Table A4. 2025 P99-tail provenance and clean-day sample sensitivity across 25 countries.

Diagnostic	Energy P99	Power P99
Countries with ≥1 imputed-input day in upper tail	8 of 25	8 of 25
Upper-tail days containing imputation, summed across countries	16	15
Minimum national change after clean-day exclusion (%)	−7.56	−16.12
Maximum national change after clean-day exclusion (%)	+2.81	+4.14

The tail diagnostics identify potential sensitivity to reconstruction and sample composition, not a measured bias in reconstructed extremes. A controlled blocked gap-injection experiment would require masking originally observed extreme blocks, rerunning the complete reconstruction pipeline and comparing reconstructed and observed tail metrics; that experiment is not presented as completed here.

Appendix A.5. Battery Power-to-Energy Ratio and Modeled Operating Intensity

Figure A2 retains the original 2025 operating-intensity comparison. Equivalent C-rate ranges from approximately 0.14 to 0.23 C, while discharge-based equivalent full-cycle intensity ranges from 60.24 to 189.67 EFC/year-equivalent. These quantities are derived from the baseline requested dispatch and P99 nameplate benchmarks, not from electrochemical cycle counting under a lifetime-aware controller. They neither predict capacity fade nor establish battery life.

Appendix A.6. Reference-Rule and Parameter-Distribution Sensitivity

The residual-load reference is part of the service definition, not a neutral estimator. Table A5 contrasts the original daily median with alternatives using the same 2025 country sample. The zero-reference case yields no active two-sided shifting service for several countries and should not be treated as a competing optimum. The median of country-level percentage changes is not generally the percentage change between the two cross-country medians.

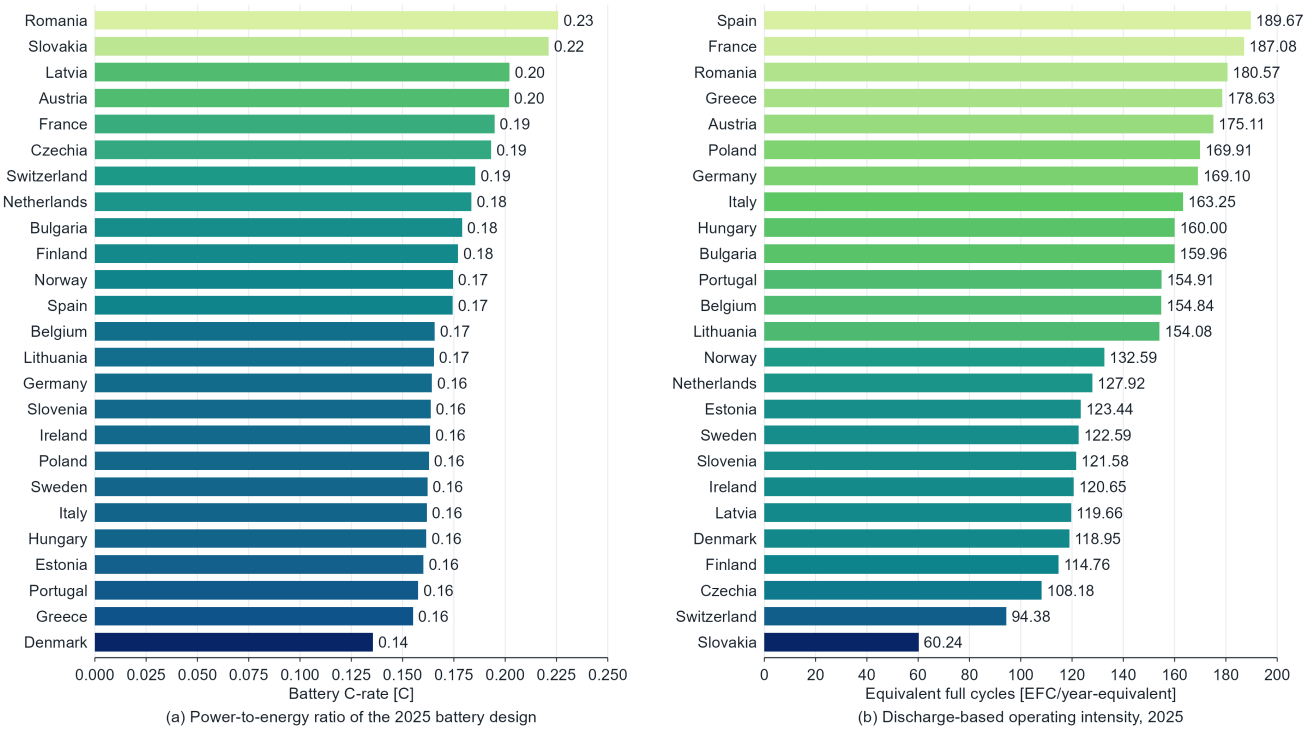


Figure A2. Battery-specific operating characteristics of the deterministic 2025 sizing framework: (**a**) implied power-to-energy ratio in C; (**b**) annualized discharge throughput expressed as EFC per 365-complete-day equivalent. Neither indicator estimates electrochemical degradation or lifetime.

Table A5. 2025 reference-rule sensitivity (medians across the S25 country sample).

Daily Residual-Load Reference	Median Nameplate Energy/Mean Load (h)	Countries with Active Service
Daily median (Q50; baseline)	2.239	25
Daily mean	2.703	25
Daily Q40	2.484	25
Daily Q60	2.116	25
Zero reference (degenerate diagnostic)	0.000	10

The original Monte Carlo analysis used 2000 draws with the stated discrete parameter probabilities and triangular usable-SOC range. Additional draws with alternative level weights and deliberately wider parameter bounds give the results in Table A6. Each row is a separately specified sensitivity distribution, not a sampling confidence interval or a probabilistic forecast.

Table A6. 2025 simulated cross-country median normalized battery-energy distributions (2000 draws per assumption set).

Parameter Assumptions	Simulated Median (h)	2.5th Percentile (h)	97.5th Percentile (h)
Original parameter weights	2.256	1.693	2.691
Uniform discrete-level weights	2.239	1.661	2.728
Edge-weighted parameter levels	2.396	1.773	2.786
Wider technical stress ranges	1.956	1.070	3.007

Appendix A.7. Matched-Horizon Decomposition and Clock-Boundary Robustness

The 2025 matched complete-week analysis separates the contributions of time-block aggregation and allowable SOC excursions. Table A7 lists the cross-country medians for four distinct definitions. These comparisons use the same eligible complete-week observations but do not all apply the same balancing rule or extreme-value aggregation. Therefore, differences between tabled medians should not be interpreted as additive within-country contributions.

Table A7. 2025 four-definition decomposition on matched complete Monday–Sunday UTC weeks (25 countries).

Code	Balancing and Sizing Definition	Country Median (h of Mean Load)
A	Daily energy balance and P99 of daily energy excursions	2.240
B	Daily energy balance and P99 of weekly maximum daily excursions	2.385
C	Weekly energy balance and P99 of maximum within-week daily excursions	3.405
D	Weekly energy balance and P99 of full-week SOC excursions	5.027

The change from A to D is 124.41% when calculated from the two displayed country medians; the median of the 25 individual country-level percentage changes is 126.12%. Shifting the calendar boundary also affects some extreme estimates. The UTC 06:00 specification, for example, changes Czechia's 2025 P99 energy by +37.38% relative to UTC 00:00. Local civil-time analyses exclude non-24 h daylight-saving transition days, so their eligible hour sets need not coincide exactly with the UTC baseline. A country-specific season-stratified week-block bootstrap used 1000 draws per system and 48–51 eligible complete 2025 weeks (48 for Ireland and 51 for the other 24 countries). Across the 25 countries, the median widths of the empirical 2.5th–97.5th percentile intervals divided by the matched-sample P99 energy were 17.57% (24 h) and 17.62% (168 h); the respective maximum widths were 46.85% and 59.11%. For Germany, the observed matched-week daily P99 energy was 142.20 GWh with a resampling range of 136.10–147.96 GWh; the weekly P99 energy was 388.97 GWh with a range of 316.42–403.55 GWh. The bootstrap reflects variability under resampling of the recorded 2025 weeks and is neither the Monte Carlo parameter-sensitivity interval nor an out-of-year validation or future reliability guarantee.

Figure A3 consolidates four additional checks: (a) joint daily-envelope coverage versus fixed-capacity replay, (b) daily median versus mean reference, (c) the four temporal definitions and (d) shifted/local clock boundaries. The graph uses the original outputs of the validated supplementary scripts rather than re-estimating the baseline battery results.

Appendix A.8. Controlled Solar–Wind Profile Perturbations

Controlled 2025 experiments altered the solar share of total VRE by ±5 percentage points where feasible, or shifted the within-day wind profile by ±6 h. The matched hourly load observations and aggregate VRE energy were retained under the experiment definitions. Table A8 reports the median of country-specific percentage changes relative to each country's baseline, rather than the percentage change in cross-country capacity medians. The solar-share increase was not identifiable for Ireland within the adopted zero-baseline-solar configuration, leaving 24 comparable countries for that case.

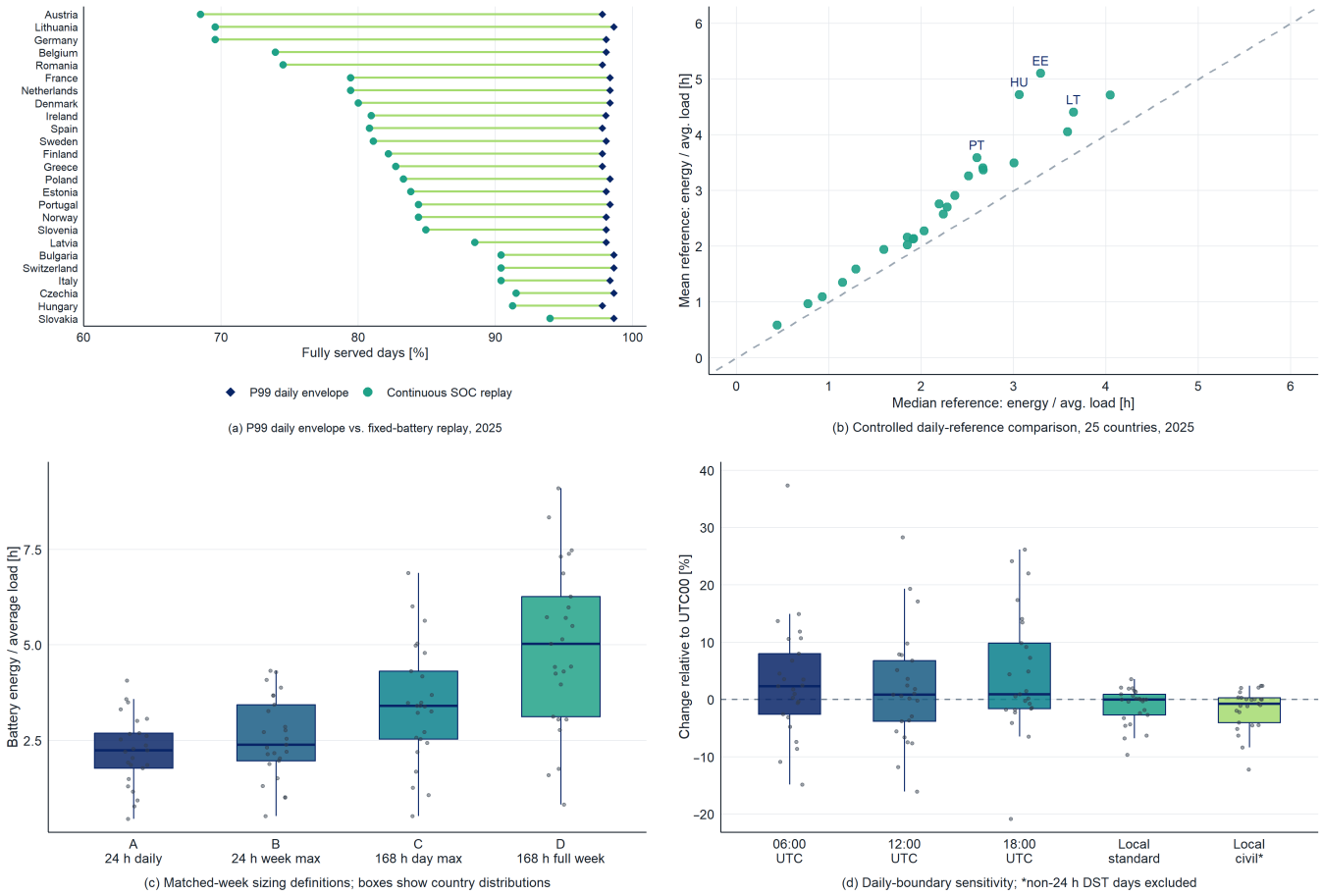


Figure A3. Additional 2025 robustness evidence. (**a**) Country-level difference between marginal P99 daily-envelope coverage and fully served days under continuous SOC replay; (**b**) nameplate energy relative to mean load under daily median versus daily mean residual-load references; (**c**) country distributions for the matched A–D temporal-service definitions; (**d**) percentage changes in P99 energy under UTC-shifted and local daily boundaries. Clock-sensitivity panels are conditional on the eligible hours of each specification; local civil-time diagnostics exclude non-24 h daylight-saving days.

Table A8. Controlled 2025 profile sensitivity of country P99 ratings relative to each national baseline.

Profile Perturbation	Countries	Median Energy Change (%)	Median Power Change (%)	Energy-Change Range (%)
Solar share −5 percentage points	25	−3.62	−1.90	−11.83 to +9.38
Solar share +5 percentage points	24	+1.37	+1.17	−8.99 to +18.73
Wind shifted −6 h within day	25	+1.22	+0.55	−11.97 to +26.13
Wind shifted +6 h within day	25	+2.28	+1.06	−7.18 to +27.94

These artificial perturbations assess the model's response to profile shape and composition; they are not forecasts, observed deployment changes or a controlled causal estimate for real national systems. The main conclusions remain conditional on the original historical data and the counterfactual dispatch rule.

References

1. Huber, M.; Dimkova, D.; Hamacher, T. Integration of Wind and Solar Power in Europe: Assessment of Flexibility Requirements. *Energy* **2014**, *69*, 236–246. https://doi.org/10.1016/j.energy.2014.02.109.
2. Jafari, M.; Botterud, A.; Sakti, A. Decarbonizing Power Systems: A Critical Review of the Role of Energy Storage. *Renew. Sustain. Energy Rev.* **2022**, *158*, 112077. https://doi.org/10.1016/j.rser.2022.112077.

3. Deguenon, L.; Yamegueu, D.; Kadri, S.M.; Gomna, A. Overcoming the Challenges of Integrating Variable Renewable Energy to the Grid: A Comprehensive Review of Electrochemical Battery Storage Systems. *J. Power Sources* **2023**, *580*, 233343. https://doi.org/10.1016/j.jpowsour.2023.233343.
4. Yang, Y.; Bremner, S.; Menictas, C.; Kay, M. Battery Energy Storage System Size Determination in Renewable Energy Systems: A Review. *Renew. Sustain. Energy Rev.* **2018**, *91*, 109–125. https://doi.org/10.1016/j.rser.2018.03.047.
5. Mallapragada, D.S.; Sepulveda, N.A.; Jenkins, J.D. Long-Run System Value of Battery Energy Storage in Future Grids with Increasing Wind and Solar Generation. *Appl. Energy* **2020**, *275*, 115390. https://doi.org/10.1016/j.apenergy.2020.115390.
6. Massucco, S.; Pongiglione, P.; Silvestro, F.; Paolone, M.; Sossan, F. Siting and Sizing of Energy Storage Systems: Towards a Unified Approach for Transmission and Distribution System Operators for Reserve Provision and Grid Support. *Electr. Power Syst. Res.* **2021**, *190*, 106660. https://doi.org/10.1016/j.epsr.2020.106660.
7. Martinez-Rico, J.; Zulueta, E.; Ruiz de Argandona, I.; Armendia, M.; Fernandez-Gamiz, U. Sizing a Battery Energy Storage System for Hybrid Renewable Power Plants Based on Optimal Market Participation under Different Market Scenarios. *IEEE Trans. Ind. Appl.* **2022**, *58*, 5624–5634. https://doi.org/10.1109/TIA.2022.3189331.
8. Moser, M.; Gils, H.C.; Pivaro, G. A Sensitivity Analysis on Large-Scale Electrical Energy Storage Requirements in Europe under Consideration of Innovative Storage Technologies. *J. Clean. Prod.* **2020**, *269*, 122261. https://doi.org/10.1016/j.jclepro.2020.122261.
9. Cebulla, F.; Naegler, T.; Pohl, M. Electrical Energy Storage in Highly Renewable European Energy Systems: Capacity Requirements, Spatial Distribution, and Storage Dispatch. *J. Energy Storage* **2017**, *14*, 211–223. https://doi.org/10.1016/j.est.2017.10.004.
10. Golombek, R.; Lind, A.; Ringkjøb, H.K.; Seljom, P. The Role of Transmission and Energy Storage in European Decarbonization towards 2050. *Energy* **2022**, *239*, 122159. https://doi.org/10.1016/j.energy.2021.122159.
11. Victoria, M.; Zhu, K.; Brown, T.; Andresen, G.B.; Greiner, M. The role of storage technologies throughout the decarbonisation of the sector-coupled European energy system. *Energy Convers. Manag.* **2019**, *201*, 111977. https://doi.org/10.1016/j.enconman.2019.111977.
12. Psarros, G.N.; Papathanassiou, S.A. Electricity Storage Requirements to Support the Transition towards High Renewable Penetration Levels: Application to the Greek Power System. *J. Energy Storage* **2022**, *55*, 105748. https://doi.org/10.1016/j.est.2022.105748.
13. Cebulla, F. Storage Demand in Highly Renewable Energy Scenarios for Europe: The Influence of Methodology and Data Assumptions in Model-Based Assessments. Ph.D. Thesis, DLR Stuttgart, Stuttgart, Germany, 2017. https://doi.org/10.18419/opus-9761.
14. Grimaldi, A.; Minuto, F.D.; Perol, A.; Casagrande, S.; Lanzini, A. Techno-economic optimization of utility-scale battery storage integration with a wind farm for wholesale energy arbitrage considering wind curtailment and battery degradation. *J. Energy Storage* **2025**, *112*, 115500. https://doi.org/10.1016/j.est.2025.115500.
15. Tejero-Gómez, J.A.; Bayod-Rújula, Á. Sizing of Battery Energy Storage Systems for Firming PV Power Including Aging Analysis. *Energies* **2024**, *17*, 1485. https://doi.org/10.3390/en17061485.
16. Moghaddam, I.N.; Chowdhury, B.; Mohajeryami, S. Predictive Operation and Optimal Sizing of Battery Energy Storage with High Wind Energy Penetration. *IEEE Trans. Ind. Electron.* **2018**, *65*, 6686–6695. https://doi.org/10.1109/TIE.2017.2774732.
17. Arévalo, P.; Cano, A.; Jurado, F. Large-Scale Integration of Renewable Energies by 2050 through Demand Prediction with ANFIS, Ecuador Case Study. *Energy* **2024**, *286*, 129446. https://doi.org/10.1016/j.energy.2023.129446.
18. Fotopoulou, M.; Tsekouras, G.J.; Rakopoulos, D.C.; Kanellos, F.D.; Kontargyri, V.T. Investment Planning Optimization for Energy Communities With Photovoltaic and Storage. *IEEE Access* **2026**, *14*, 98275–98294. https://doi.org/10.1109/ACCESS.2026.3707056.
19. European Network of Transmission System Operators for Electricity (ENTSO-E). ENTSO-E Transparency Platform. Online Database. 2026. Available online: https://transparency.entsoe.eu/ (accessed on 10 August 2026).
20. Zsiborács, H.; Baranyai, N.H.; Vincze, A.; Zentkó, L.; Birkner, Z.; Máté, K.; Pintér, G. Intermittent Renewable Energy Sources: The Role of Energy Storage in the European Power System of 2040. *Electronics* **2019**, *8*, 729. https://doi.org/10.3390/electronics8070729.
21. Zsiborács, H.; Pintér, G.; Vincze, A.; Birkner, Z.; Baranyai, N.H. Grid balancing challenges illustrated by two European examples: Interactions of electric grids, photovoltaic power generation, energy storage and power generation forecasting. *Energy Rep.* **2021**, *7*, 3805–3818. https://doi.org/10.1016/j.egyr.2021.06.007.
22. Jaradat, T.; Khatib, T. A Review of Battery Energy Storage System for Renewable Energy Penetration in Electrical Power System: Environmental Impact, Sizing Methods, Market Features, and Policy Frameworks. *Future Batter.* **2025**, *7*, 100106. https://doi.org/10.1016/j.fub.2025.100106.
23. Deliu, A.D.; Cazacu, E. A Comprehensive Review of Utility-Scale Battery Energy Storage: Technologies, Control Strategies, Planning Methods, and Future Directions. *Tech. Rom. J. Appl. Sci. Technol.* **2025**, *30*, 252–261. https://doi.org/10.47577/technium.v30i.13230.

24. Khan, A.A.; Minai, A.; Godi, R.; Sharma, V.S.; Malik, H.; Afthanorhan, A. Optimal Sizing, Techno-Economic Feasibility and Reliability Analysis of Hybrid Renewable Energy System: A Systematic Review of Energy Storage Systems' Integration. *IEEE Access* **2025**, *13*, 59198–59226. https://doi.org/10.1109/ACCESS.2025.3535520.
25. Odero, H.; Wekesa, C.; Irungu, G. Comprehensive Review of Energy Storage Technologies: Types, Applications, Optimal Sizing and Siting in Power Systems. In Proceedings of the 2022 IEEE PES/IAS PowerAfrica, Kigali, Rwanda, 22–26 August 2022. https://doi.org/10.1109/PowerAfrica53997.2022.9905263.
26. Safarzadeh, H.; Jahanbakhshi, M.; Di Maria, F.; Javani, N. Battery Energy Storage Systems in Power Systems: A Comprehensive Systematic Review of Technologies, Applications, and Challenges. *Int. J. Energy Res.* **2026**, *2026*, 5573003. https://doi.org/10.1155/er/5573003.
27. Areola, R.; Adebiyi, A.; Moloi, K. Integrated Energy Storage Systems for Enhanced Grid Efficiency: A Comprehensive Review of Technologies and Applications. *Energies* **2025**, *18*, 1848. https://doi.org/10.3390/en18071848.
28. Heredia, F.; Cuadrado, M.D.; Corchero, C. On Optimal Participation in the Electricity Markets of Wind Power Plants with Battery Energy Storage Systems. *Comput. Oper. Res.* **2018**, *96*, 316–329. https://doi.org/10.1016/j.cor.2018.03.004.
29. Faessler, B.; Bogunović Jakobsen, A. Autonomous Operation of Stationary Battery Energy Storage Systems—Optimal Storage Design and Economic Potential. *Energies* **2021**, *14*, 1333. https://doi.org/10.3390/en14051333.
30. Kelly, J.J.; Leahy, P.G. Optimal investment timing and sizing for battery energy storage systems. *J. Energy Storage* **2020**, *28*, 101272. https://doi.org/10.1016/j.est.2020.101272.
31. Fathima, H.; Palanisamy, K. Optimized Sizing, Selection, and Economic Analysis of Battery Energy Storage for Grid-Connected Wind-PV Hybrid System. *Model. Simul. Eng.* **2015**, *2015*, 713530. https://doi.org/10.1155/2015/713530.
32. Saez-de Ibarra, A.; Martinez-Laserna, E.; Stroe, D.I.; Swierczynski, M.; Rodriguez, P. Sizing Study of Second Life Li-ion Batteries for Enhancing Renewable Energy Grid Integration. *IEEE Trans. Ind. Appl.* **2016**, *52*, 4999–5008. https://doi.org/10.1109/tia.2016.2593425.
33. Weniger, J.; Tjaden, T.; Quaschning, V. Sizing of Residential PV Battery Systems. *Energy Procedia* **2014**, *46*, 78–87. https://doi.org/10.1016/J.EGYPRO.2014.01.160.
34. Hesse, H.; Martins, R.; Musílek, P.; Naumann, M.; Truong, C.; Jossen, A. Economic Optimization of Component Sizing for Residential Battery Storage Systems. *Energies* **2017**, *10*, 835. https://doi.org/10.3390/EN10070835.
35. Terlouw, T.; AlSkaif, T.; Bauer, C. Techno-Economic Assessment of PV-Coupled Battery Energy Storage Systems with Different Sizing Methodologies. In Proceedings of the 2021 IEEE Madrid PowerTech, Madrid, Spain, 28 June–2 July 2021; pp. 1–6. https://doi.org/10.1109/powertech46648.2021.9494881.
36. Kumar, J.; Parthasarathy, C.; Västi, M.; Laaksonen, H.; Shafiekhah, M.; Kauhaniemi, K. Sizing and Allocation of Battery Energy Storage Systems in Åland Islands for Large-Scale Integration of Renewables and Electric Ferry Charging Stations. *Energies* **2020**, *13*, 317. https://doi.org/10.3390/en13020317.
37. Dulout, J.; Jammes, B.; Alonso, C.; AnvariMoghaddam, A.; Luna, A.; Guerrero, J. Optimal sizing of a lithium battery energy storage system for grid-connected photovoltaic systems. In Proceedings of the IEEE International Conference on DC Microgrids, Nuremburg, Germany, 27–29 June 2017. https://doi.org/10.1109/ICDCM.2017.8001106.
38. Koubar, M.; Lindberg, O.; Lingfors, D.; Huang, P.; Berg, M.; Munkhammar, J. Techno-economical assessment of battery storage combined with large-scale Photovoltaic power plants operating on energy and Ancillary Service Markets. *Appl. Energy* **2025**, *382*, 125200. https://doi.org/10.1016/j.apenergy.2024.125200.
39. Tauš, P.; Taušová, M.; Sivák, P.; Shejbalová Muchová, M.; Mihaliková, E. Parameter Optimization Model Photovoltaic Battery System for Charging Electric Cars. *Energies* **2020**, *13*, 4497. https://doi.org/10.3390/en13174497.
40. Kwon, K.; Lee, H.B.; Kim, N.; Park, S.; Joshua, S. Integrated Battery and Hydrogen Energy Storage for Enhanced Grid Power Savings and Green Hydrogen Utilization. *Appl. Sci.* **2024**, *14*, 7631. https://doi.org/10.3390/app14177631.
41. Wang, G.; Blondeau, J. Optimal combination of daily and seasonal energy storage using battery and hydrogen production to increase the self-sufficiency of local energy communities. *J. Energy Storage* **2024**, *92*, 112206. https://doi.org/10.1016/j.est.2024.112206.
42. Secchi, M.; Barchi, G.; Macii, D.; Moser, D.; Petri, D. Multi-objective battery sizing optimisation for renewable energy communities with distribution-level constraints: A prosumer-driven perspective. *Appl. Energy* **2021**, *297*, 117171. https://doi.org/10.1016/j.apenergy.2021.117171.
43. Guezgouz, M.; Jurasz, J.; Bekkouche, B.; Ma, T.; Javed, M.; Kies, A. Optimal hybrid pumped hydro-battery storage scheme for off-grid renewable energy systems. *Energy Convers. Manag.* **2019**, *199*, 112046. https://doi.org/10.1016/j.enconman.2019.112046.
44. Castillejo-Cuberos, A.; Cardemil, J.; Escobar, R. Techno-economic assessment of photovoltaic plants considering high temporal resolution and non-linear dynamics of battery storage. *Appl. Energy* **2023**, *334*, 120712. https://doi.org/10.1016/j.apenergy.2023.120712.
45. Pizzuti, I.; Delibra, G. Integration of battery energy storage systems in renewable energy communities: Optimal configurations and strategies. *J. Energy Storage* **2026**, *153*, 120857. https://doi.org/10.1016/j.est.2026.120857.

46. Eroğlu, H.; Kurtuluş, O. Strategic design of wind energy and battery storage for efficient and sustainable energy systems. *Sci. Rep.* **2025**, *15*, 34976. https://doi.org/10.1038/s41598-025-18863-5.
47. Mykhei, M.; Melnychenko, D.; Tauš, P.; Taušová, M. Rooftop Bifacial Photovoltaics Under Site-Specific Roof-Albedo and Geometry Scenarios: Energy, Emission, and Economic Assessment. *Sustainability* **2026**, *18*, 7561. https://doi.org/10.3390/su18157561.
48. Després, J.; Mima, S.; Kitous, A.; Criqui, P.; Hadjsaid, N.; Noirot, I. Storage as a flexibility option in power systems with high shares of variable renewable energy sources: A POLES-based analysis. *Energy Econ.* **2017**, *64*, 638–650. https://doi.org/10.1016/j.eneco.2016.03.006.
49. Garwa, A.; Pascual, J.; Marroyo, L. Complementing Hydroelectric Power with Batteries for the Spanish Electric System. In Proceedings of the IEEE PES Innovative Smart Grid Technologies Conference Europe, Valletta, Malta, 20–23 October 2025. https://doi.org/10.1109/ISGTEurope64741.2025.11305436.
50. Jin, L.; Rossi, M.; Ferrario, A.M.; Alberizzi, J.C.; Renzi, M.; Comodi, G. Integration of battery and hydrogen energy storage systems with small-scale hydropower plants in off-grid local energy communities. *Energy Convers. Manag.* **2023**, *286*, 117019. https://doi.org/10.1016/j.enconman.2023.117019.
51. Mensik, J.; Wöss, D.; Schmidt, J.; Pröll, T. Deductive assessment of a hybrid electricity storage system depending on varying renewable generation designs for Austria. *Energy Rep.* **2025**, *13*, 514–524. https://doi.org/10.1016/j.egyr.2024.12.026.
52. Miranda, I.; Silva, N.; Leite, H. A Holistic Approach to the Integration of Battery Energy Storage Systems in Island Electric Grids With High Wind Penetration. *IEEE Trans. Sustain. Energy* **2016**, *7*, 775–785. https://doi.org/10.1109/TSTE.2015.2497003.
53. Bussar, C.; Stöcker, P.; Cai, Z.; Moraes, L.; Alvarez, R.; Chen, H.; Breuer, C.; Moser, A.; Leuthold, M.; Sauer, D. Large-scale Integration of Renewable Energies and Impact on Storage Demand in a European Renewable Power System of 2050. *Energy Procedia* **2015**, *73*, 145–153. https://doi.org/10.1016/J.EGYPRO.2015.07.662.
54. Frate, G.F.; Carro, P.P.; Ferrari, L.; Desideri, U. Techno-economic sizing of a battery energy storage coupled to a wind farm: An Italian case study. *Energy Procedia* **2018**, *148*, 447–454. https://doi.org/10.1016/J.EGYPRO.2018.08.119.
55. González-González, J.M.; Martín, S.; López, P.; Aguado, J.A. Hybrid battery-ultracapacitor storage system sizing for renewable energy network integration. *Iet Renew. Power Gener.* **2020**, *14*, 2367–2375. https://doi.org/10.1049/iet-rpg.2019.1310.
56. Vazquez-Rodriguez, A.; Michiorri, A.; Kariniotakis, G. Integrating thermal properties and degradation modelling of batteries into the scheduling of hybrid power plants with photovoltaics. *J. Energy Storage* **2023**, *73*, 108782. https://doi.org/10.1016/j.est.2023.108782.
57. Khosravi, N.; Çelik, D.; Sepehrzad, R.; Oubelaid, A.; Abdolmohammadi, H.; Al-Durra, A. A comprehensive review of battery and hydrogen storage systems across technical, economic, and environmental dimensions. *J. Energy Storage* **2026**, *170*, 122821. https://doi.org/10.1016/j.est.2026.122821.
58. Pous Cabello, J.; Mykhei, M.; Pantelakis, D.; Amez, I.; Taušová, M.; Tauš, P. Estimation of the Potential for Green Hydrogen Production from Untapped Renewable Energy Sources in Spain in 2024. *Appl. Sci.* **2025**, *15*, 11873. https://doi.org/10.3390/app152211873.
59. Amez, I.; León, D.; Ivannikov, A.; Kolikov, K.; Castells, B. Potential of CBM as an Energy Vector in Active Mines and Abandoned Mines in Russia and Europe. *Energies* **2023**, *16*, 1196. https://doi.org/10.3390/en16031196.
60. Amez, I.; Castells, B.; León, D.; Paredes, R. Study of Quaternary Hydrogen and Biogas Mixtures: An Industrial Safety Approach. *Fuel* **2025**, *381*, 133663. https://doi.org/10.1016/j.fuel.2024.133663.
61. Zsiborács, H.; Baranyai, N.; Zentkó, L.; Mórocz, A.; Pócs, I.; Mate, K.; Pintér, G. Electricity Market Challenges of Photovoltaic and Energy Storage Technologies in the European Union: Regulatory Challenges and Responses. *Appl. Sci.* **2020**, *10*, 1472. https://doi.org/10.3390/app10041472.
62. Tejero-Gómez, J.A.; Bayod-Rújula, Á.A. Analysis of Photovoltaic Plants with Battery Energy Storage Systems (PV-BESS) for Monthly Constant Power Operation. *Energies* **2023**, *16*, 4909. https://doi.org/10.3390/en16134909.
63. Migliari, L.; Micheletto, D.; Marchionni, M.; Petrollese, M.; Cau, G.; Cocco, D. AN ANALYSIS OF EU POWER SYSTEM FLEXIBILITY: STORAGE CAPACITY NEEDS UNDER INCREASING VARIABLE RENEWABLE ENERGY SOURCES (VRES) PENETRATION. In Proceedings of the 37th International Conference on Efficiency, Cost, Optimization, Simulation and Environmental Impact of Energy Systems (ECOS 2024), Rhodes, Greece, 30 June–5 July 2024; pp. 1842–1853. https://doi.org/10.52202/077185-0158.
64. Munzke, N.; Büchle, F.; Smith, A.; Hiller, M. Influence of Efficiency, Aging and Charging Strategy on the Economic Viability and Dimensioning of Photovoltaic Home Storage Systems. *Energies* **2021**, *14*, 7673. https://doi.org/10.3390/en14227673.
65. Englberger, S.; Jossen, A.; Hesse, H. Unlocking the Potential of Battery Storage with the Dynamic Stacking of Multiple Applications. *Cell Rep. Phys. Sci.* **2020**, *1*, 100238. https://doi.org/10.1016/j.xcrp.2020.100238.
66. Zeh, A.; Müller, M.; Naumann, M.; Hesse, H.; Jossen, A.; Witzmann, R. Fundamentals of Using Battery Energy Storage Systems to Provide Primary Control Reserves in Germany. *Batteries* **2016**, *2*, 29. https://doi.org/10.3390/batteries2030029.
67. Patsios, C.; Wu, B.; Chatzinikolaou, E.; Rogers, D.J.; Wade, N.; Brandon, N.; Taylor, P. An Integrated Approach for the Analysis and Control of Grid Connected Energy Storage Systems. *J. Energy Storage* **2016**, *5*, 48–61. https://doi.org/10.1016/j.est.2015.11.011.

68. Ferrario, A.; Bartolini, A.; Manzano, F.S.; Vivas, F.; Comodi, G.; McPhail, S.; Andújar, J. A model-based parametric and optimal sizing of a battery/hydrogen storage of a real hybrid microgrid supplying a residential load: Towards island operation. *Adv. Appl. Energy* **2021**, *3*, 100048. https://doi.org/10.1016/j.adapen.2021.100048.
69. Etherden, N.; Bollen, M.H.J. Dimensioning of Energy Storage for Increased Integration of Wind Power. *IEEE Trans. Sustain. Energy* **2013**, *4*, 546–553. https://doi.org/10.1109/TSTE.2012.2228244.
70. Chung, C.; Wen, F.; Ledwich, G.; Venkatesh, B. Optimal utilisation of storage systems in transmission and distribution systems. *Iet Gener. Transm. Distrib.* **2016**, *10*, 563–565. https://doi.org/10.1049/IET-GTD.2016.0114.
71. Kácsor, E.; Mezősi, A.; Szabó, L. Integrating solar plants into the European power grid—What is the optimal capacity combination of PV and battery storage? *Energy Convers. Manag. X* **2025**, *26*, 101029. https://doi.org/10.1016/j.ecmx.2025.101029.
72. de la Torre, S.; González-González, J.; Aguado, J.; Martín, S. Optimal Battery Sizing Considering Degradation for Renewable Energy Integration. *IET Renew. Power Gener.* **2019**, *13*, 572–577. https://doi.org/10.1049/IET-RPG.2018.5489.
73. Vasylyev, A.; Vannoni, A.; Sorce, A. Optimal Dispatch of Li-Ion Battery Energy Storage, Reviewing and Considering Cycling and Calendar Ageing Models. *Appl. Therm. Eng.* **2025**, *265*, 125597. https://doi.org/10.1016/j.applthermaleng.2025.125597.
74. Wüllner, J.; Reiners, N.; Millet, L.; Salibi, M.; Stortz, F.; Vetter, M. Review of Stationary Energy Storage Systems Applications, Their Placement, and Techno-Economic Potential. *Curr. Sustain. Energy Rep.* **2021**, *8*, 263–273. https://doi.org/10.1007/s40518-021-00188-2.
75. Ezennaya, S.O.; Kowal, J. A Parametric LFP Battery Degradation Model for Techno-Economic Assessment of European System-Imbalance Services. *Batteries* **2026**, *12*, 56. https://doi.org/10.3390/batteries12020056.
76. Mykhei, M.; Domaracka, L.; Taušová, M.; Saffova, D.; Tauš, P.; Kowal, B.; Alkhalaf, I. The Evolution of Renewable Energy Sources in the Visegrad Four Countries: A Comparative Study of Trends and Policies. *Energies* **2025**, *18*, 5907. https://doi.org/10.3390/en18225907.
77. Taušová, M.; Mykhei, M.; Culkova, K.; Tauš, P. Comparison of Renewable Energy Implementation in Geographically and Climatically Diverse Regions. *Sustainability* **2025**, *17*, 3098. https://doi.org/10.3390/su17073098.
78. Mykhei, M.; Pantelakis, D.; Pous Cabello, J.; Amez, I.; Taušová, M.; Tauš, P. A Quantitative Analysis of the Impact of Support Policies on the Share of Renewable Energy in Europe. *Sustainability* **2026**, *18*, 1725. https://doi.org/10.3390/su18041725.
79. Mykhei, M.; Domaracká, L.; Taušová, M.; Šaffová, D.; Tauš, P. The Gap in Renewable Energy Between the V4 and the EU Average: An Empirical Comparison by Sector and Technology. *Energies* **2026**, *19*, 1585. https://doi.org/10.3390/en19061585.
80. Slyvkanych, N. Decoding National Genius: Efficiency of Intellectual Capital Utilisation in the European Union. *J. Appl. Econ. Sci.* **2025**, *20*, 875–894. https://doi.org/10.57017/jaes.v20.4(90).14.
81. Dancakova, D.; Glova, J.; Andrejovska, A. The Robust Efficiency Estimation in Lower Secondary Education: Cross-Country Evidence. *Mathematics* **2021**, *9*, 3249. https://doi.org/10.3390/math9243249.
82. Glova, J.; Bernatik, W.; Dancakova, D. Assessment of Changes in Country Risk Clustering of the EU Countries. *AD ALTA J. Interdiscip. Res.* **2019**, *9*, 47–53.
83. Mykhei, M.; Marasova, D., Jr.; Bobinics, B.; Marasova, D.; Taušová, M.; Kudelas, D. Probabilistic Assessment of Downtime-Related Energy-Service Unavailability, Production Loss and Economic Impact in Continuous Material-Handling Systems. *Appl. Sci.* **2026**, *16*, 5697. https://doi.org/10.3390/app16115697.
84. Mykhei, M.; Bobinics, B.; Marasova, D.; Taušová, M.; Kudelas, D.; Marasova, D., Jr. Frequency–Severity Asymmetry and Regime-Based Forecasting of Operational Downtime in Continuous Material-Handling Systems. *Mathematics* **2026**, *14*, 1857. https://doi.org/10.3390/math14111857.
85. Eurostat. Population Change—Demographic Balance and Crude Rates at National Level (Demo_Gind). Eurostat Online Database. 2026. Available online: https://ec.europa.eu/eurostat/databrowser/view/demo_gind/default/table?lang=en (accessed on 10 August 2026).
86. World Bank. Population, Total (SP.POP.TOTL). World Development Indicators. 2026. Available online: https://data.worldbank.org/indicator/SP.POP.TOTL (accessed on 10 August 2026).
87. Budova, J.; Sulikova, V.; Sinicakova, M. When Inflation Again Matters: Do Domestic and Global Output Gaps Determine Inflation in the EU? *Amfiteatru Econ.* **2023**, *25*, 575–592. https://doi.org/10.24818/EA/2023/63/575.
88. Budova, J.; Sulikova, V.; Sinicakova, M. Inflation Synchronisation Strengthening in Europe in Post-Quantitative Easing and Post-Pandemic High Inflation Times: Consequences for Single Monetary Policy Management. *Management* **2023**, *27*, 121–148. https://doi.org/10.58691/man/176596.
89. Sorourifar, F.; Zavala, V.; Dowling, A. Integrated Multiscale Design, Market Participation, and Replacement Strategies for Battery Energy Storage Systems. *IEEE Trans. Sustain. Energy* **2020**, *11*, 84–92. https://doi.org/10.1109/TSTE.2018.2884317.
90. Chen, Y.; Zhu, M.; Chen, M. Comprehensive Experimental Research on Wrapping Materials Influences on the Thermal Runaway of Lithium-Ion Batteries. *Emerg. Manag. Sci. Technol.* **2025**, *5*, e007. https://doi.org/10.48130/emst-0025-0005.

91. Yang, J.; Ling, Z.; Wang, J.; Chen, B.; Li, L.; Han, C.; Wang, Z.; Wang, J. Thermo-Electrical Coupling-Induced Thermal Runaway Evolution, Multphysical Failure and Dynamic Warning Strategy of Large-Format LiFePO4 Batteries. *Energy Storage Mater.* **2026**, *91*, 105573. https://doi.org/10.1016/j.ensm.2026.105573.
92. Li, S.; Sun, X.; Chen, B.; He, X.; Ling, Z.; Huang, Y.; Wang, J.; Wang, Z.; Wang, J. Thermal Runaway Jet Flames of Lithium Iron Phosphate Batteries under Inclined Ceilings: Flame Dynamics, Ceiling Thermal Exposure, and Safety Evaluation. *Appl. Therm. Eng.* **2026**, *307*, 133417. https://doi.org/10.1016/j.applthermaleng.2026.133417.
93. Xu, Q.; Jia, S.; Li, Y.; Wang, H.; Guo, M.; Zhou, S.; Yang, X.; Li, C.; Tu, H.; Zhu, H.; et al. Revealing the Critical Role of Amide Bonds in Pore Structure and Interfacial Stability of Hard Carbon Anodes for Sodium-Ion Batteries. *Adv. Funct. Mater.* **2026**, *36*, e76601. https://doi.org/10.1002/adfm.76601.
94. Pavolová, H.; Seňová, A.; Bakalár, T. Increase of Alternative and Renewable Energy Sources Utilization in Slovakia by 2020 in Comparison to Other Selected EU Countries. *Appl. Mech. Mater.* **2012**, *152–154*, 495–500. https://doi.org/10.4028/www.scientific.net/AMM.152-154.495.
95. Taušová, M.; Domaracká, L.; Čulková, K.; Tauš, P.; Kaňuch, P. Development of Energy Poverty and Its Solutions through the Use of Renewables: The EU Case with a Focus on Slovakia. *Energies* **2024**, *17*, 3762. https://doi.org/10.3390/en17153762.
96. Mihaliková, E.; Štuller, T. Ekonomické nástroje verejnej politiky zamerané na životné prostredie. *Acta Oeconomica Cassoviensia* **2024**, *17*, 40–50.
97. Mihaliková, E.; Taušová, M.; Čulková, K. Public Expenses and Investment in Environmental Protection and Its Impact on Waste Management. *Sustainability* **2022**, *14*, 5270. https://doi.org/10.3390/su14095270.
98. Glova, J.; Slyvkanyč, N. Impact of ESG Subset Performance on Financial and Market Outcomes. *AD ALTA J. Interdiscip. Res.* **2024**, *14*, 56–58.
99. Mihaliková, E.; Štuller, T. Umelá inteligencia a jej možnosti využitia pri budovaní inteligentných miest. *Verejná Správa Regionálny rozvoj/Ekonómia Manažment Mark.* **2025**, *21*, 114–124.
100. Štuller, T. Citizen Science ako nástroj environmentálnej politiky v ére umelej inteligencie. In *AI vo Verejnej Správe: Výzvy, Príležitosti a Riešenia*; Douša, M., Ed.; Univerzita Pavla Jozefa Šafárika v Košiciach, Vydavateľstvo ŠafárikPress: Košice, Slovakia, 2026; pp. 9–19.
101. Šaffová, D.; Petráš, D.; Mykhei, M. Implementation of the Models of Operational Research for the Solution of the CNC Machines Life Cycle. *Manag. Syst. Prod. Eng.* **2025**, *33*, 289–297. https://doi.org/10.2478/mspe-2025-0028.
102. Teplická, K.; Straka, M. Sustainability of Extraction of Raw Material by a Combination of Mobile and Stationary Mining Machines and Optimization of Machine Life Cycle. *Sustainability* **2020**, *12*, 10454. https://doi.org/10.3390/su122410454.
103. Malindžák, D.; Mihaliková, E.; Pandula, B. Heuristic Model for Production Scheduling Wide-Strip Rolling Mill. *Metalurgija* **2019**, *58*, 117–119.
104. Bobinics, B.; Marasová, D.; Bindzár, P. Comparison of a Conventional and Pipe Conveyor in Terms of Their Energy Efficiency Using Simulation Modeling. *Min. Sci.* **2025**, *32*, 223–239. https://doi.org/10.37190/msc/215173.
105. Slyvkanyc, N.; Glova, J.; Andrejovska, A.; Barski, R. Intellectual Capital Meets Industry 4.0: Transforming Logistics through Bibliometric Insights. *Acta Logist.* **2024**, *11*, 505–516. https://doi.org/10.22306/al.v11i4.443.

Disclaimer/Publisher's Note: The statements, opinions and data contained in all publications are solely those of the individual author(s) and contributor(s) and not of MDPI and/or the editor(s). MDPI and/or the editor(s) disclaim responsibility for any injury to people or property resulting from any ideas, methods, instructions or products referred to in the content.